VEÐURSTOFA ÍSLANDS

Report
06005

Ragnar Stefánsson
Maurizio Bonafede
Frank Roth
Páll Einarsson
Þóra Árnadóttir
Gunnar B. Guðmundsson

Modelling and parameterizing the Southwest Iceland earthquake release and deformation process

VÍ-ES-03
Reykjavík
Febrúar 2006

Contents

1 Introduction

The South Iceland Seismic Zone (SISZ) has for a long time been considered the area of Iceland where the largest earthquake hazards are to be expected. Much research has been carried out during the last 2 to 3 decades to try to understand the ongoing earthquake processes with the hope to be able to make useful warnings ahead of large earthquakes. Monitoring systems have been built in the area for better observing it. Among results of these efforts is that it was possible to make a useful short-term warning ahead of the second of the two June 2000 earthquakes in the SISZ. The ongoing PREPARED-project is a multidisciplinary project to collect the experiences gained in the June 2000 earthquakes and for modelling the processes with the aim of enhancing hazard assessments and warnings for dangerous earthquakes (Stefánsson et al. 2002).

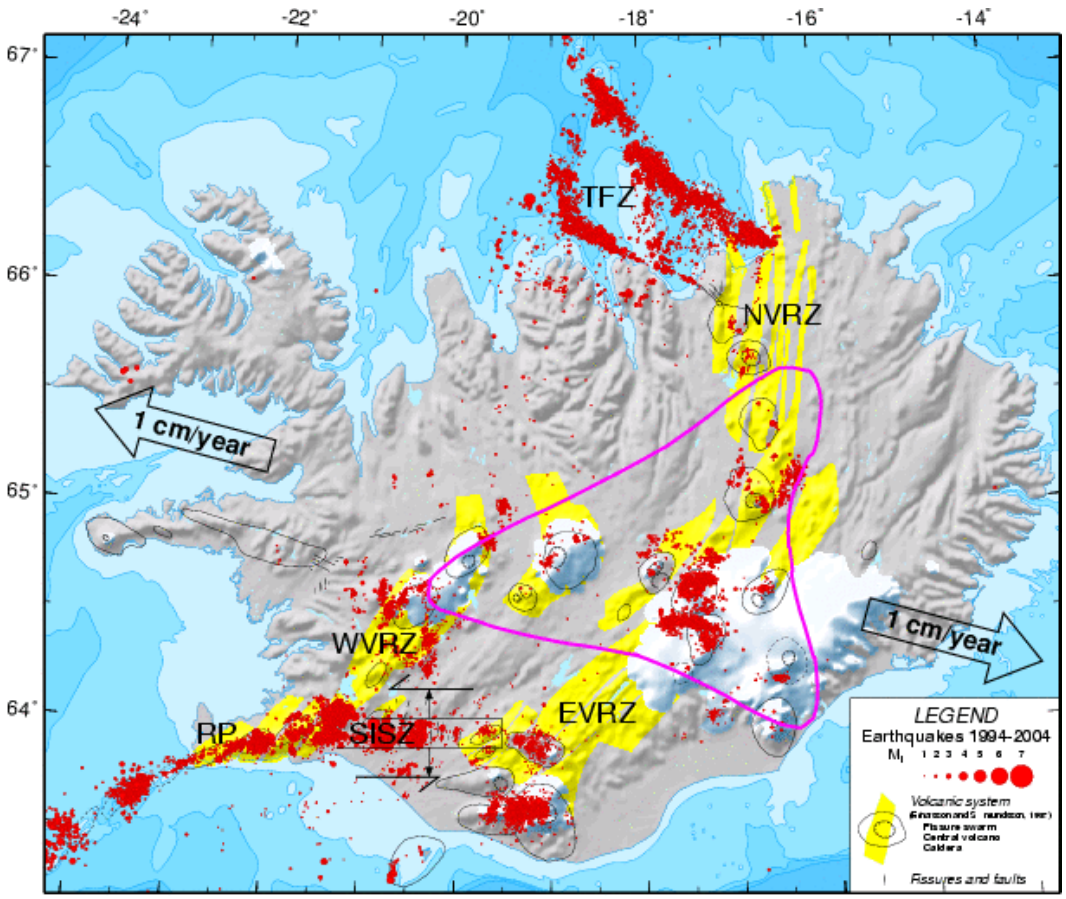

Figure 1. *The South Iceland Seismic Zone (SISZ), Reykjanes Peninsula (RP), plate motion directions, transform motion along SISZ and opening are indicated. The outlines of the Iceland plume (hotspot) at 300-400 km depth are shown by the purple contour.*

The westward prolongation of the SISZ is on the Reykjanes Peninsula (RP) (Figure 1) where destructive earthquakes also occur. Even if its tectonic character is different from SISZ it is necessary to deal with SISZ and RP as a whole, as well as with the adjacent volcanoes and rift zones.

The main focus of this report is, however, the SISZ.

2 The plate tectonic framework

The earthquakes of June 2000 occurred within SISZ, a left-lateral transform zone, which is a branch of the mid-Atlantic plate boundary that crosses Iceland and separates the two major lithospheric plates, the Eurasia Plate to the east and the North America Plate to the west. Offshore, to the north and south of Iceland, the boundary is relatively simple. It follows the Kolbeinsey and Reykjanes Ridges respectively, but on land the situation is more complex. The plate boundary on Iceland is expressed by a series of seismic and volcanic zones. Two transform zones connect the presently active Northern and Eastern Volcanic Rift Zones (NVRZ and EVRZ respectively) to the ridges offshore (Einarsson 1991). The relative plate motion across the ridge is estimated 18.9 mm/+-0.5 mm/year in direction 102.9°+-1.1° east of north (DeMets et al. 1990; DeMets et al. 1994) (Figure 1).

The SISZ is almost due EW so the plate motion vector according to DeMets et al. (1990) and DeMets et al. (1994) would be approximately 1.8 cm/year parallel to the zone and there would be a NS opening of only 0.5 cm/year in the long run. The Reykjanes Peninsula is striking 70º west of south and has thus a significant opening component.

The structure and the activity of the plate boundary are strongly influenced by the Iceland Plume beneath Central Iceland (Tryggvason et al. 1983; Stefánsson and Halldórsson 1988) (Figure 1). The relative motion of the plate boundary with respect to the plume leads to ridge jumps, propagating rifts, oblique rifts, and other complexities. A new rift zone is initiated when the old rift has migrated some critical distance off the plume center. Over geological times the transform zones connecting the rifts are unstable and respond to changes in the configuration of the rifts.

At least two rift jumps have occurred in the southern part of Iceland during the last 7 million years. The first one occurred 6-7 million years ago when the Western Volcanic Rift Zone became active and took over from the Snæfellsnes Rift Zone (Kristjánsson and Jónsson 1998; Khodayar and Einarsson 2002). The EVRZ became active 3 million years ago, replacing the WVRZ. This rift jump is still in progress (Sigmundsson et al. 1995). Both rifts show definite signs of recent activity. GPS geodetic measurements show that most of the spreading is occurring across the Eastern Rift, with about 10% taken up across the Western Rift at the present time, i.e. during the last decade or so (Geirsson et al. 2006; LaFemina et al. 2005). The SISZ, where the two large earthquakes of year 2000 occurred, is a transform zone between these two rifts as seen in Figure 1.

The plate boundary in Iceland is in several ways different from that in the adjacent oceanic areas. The zone occupied by plate boundary structures is wider, most likely reflecting the intensive magma production of the Icelandic hotspot (plume). Furthermore, the plate boundary has branches, sometimes parallel or subparallel, reflecting its unstable geometry. The boundary zones can be divided into segments, each one with relatively homogeneous characteristics, but different from adjacent segments. The main characteristics are rate of volcanism, type of volcanic structures, petrological signatures, type and intensity of faulting and fissuring, rate of seismicity, arrangement of fault structures with respect to the segment and the direction of spreading. It should be mentioned at this point that there is a considerable confusion in the literature regarding the definition, demarcation, and names of the different branches of the active zones and plate boundaries in Iceland.

2.1 The Reykjanes Peninsula Oblique Rift

The Reykjanes Peninsula Oblique Rift is a structural continuation of the Reykjanes Ridge, which is an obliquely spreading part of the mid-Atlantic plate boundary. The tectonic structure of the northern Reykjanes Ridge and the Reykjanes Peninsula is characterized by volcanic systems that are arranged en echelon along the plate boundary (Figure 2). Their central volcanoes are immature, have for example neither developed significant amount of acidic magma nor calderas. The degree of obliqueness of the boundary increases towards the east with a clear break at the tip of the peninsula. The segment has an overall trend of about 70° and a total length of 70 km, from the tip of the peninsula to the Hengill triple junction near 21.5°W. The plate boundary is marked by a narrow zone of seismicity. The fissure swarms of the volcanic systems are oblique to the boundary and extend a few tens of kilometers into the plates on either side. Less conspicuous, but probably equally important, are strike-slip faults that cut across the plate boundary at a high angle, often close to perpendicular. Earthquake fault plane solutions show a consistent direction of the least compressive stress, horizontal and NW-SE.

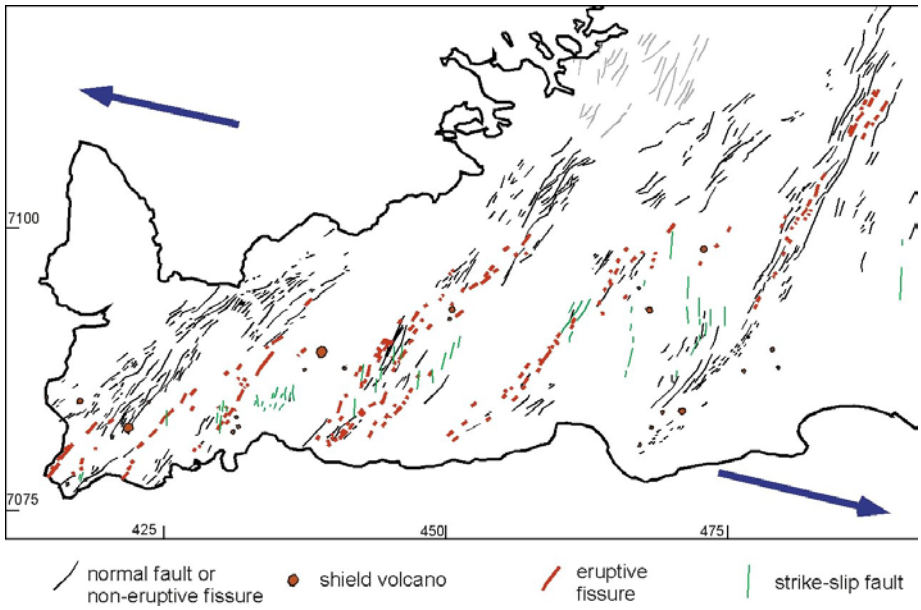

Figure 2. *Structural elements of the Reykjanes Peninsula Oblique Rift.*

The style of seismic strain release changes systematically along the peninsula, from being quite swarmlike in the western part to more strike-slip character towards east.

The fissure swarms on the Reykjanes Peninsula occupy a much wider zone than the epicentral belt. They have the general structure of shallow grabens, and are structurally identical to other fissure swarms of the divergent plate boundaries in Iceland, including the Krafla fissure swarm. It is therefore natural to interpret them in a similar way, as the result of repeated dyke injection into the crust.

Two types of volcanic structures dominate the activity, fissure eruptions and monogenetic lava shields (Figure 2). Most of the shields were active during early Holocene, following the deloading of the crust when the Pleistocene ice sheets disappeared.

Crustal deformation along the plate boundary on the Reykjanes Peninsula appears to occur in two different modes: (1) dry or seismic mode, and (2) wet or magmatic mode.

Deformation in the dry mode occurs during periods when magma is not available to the crust in any appreciable quantity, and faulting takes place mostly on the NS faults. In the magmatic mode magma is injected along the NE-trending fissure swarms and the fracturing expected is mostly on fissures and normal faults.

At present times we are in a dry seismic activity period. The seismic activity is episodic on the time scale of decades. The magmatic activity periods are also episodic, but on a much longer time scale. The latest major magmatic episode occurred in the tenth to thirteenth centuries and no eruptions have taken place on the peninsula since 1240.

2.2 The South Iceland Seismic Zone

The gap between the two subparallel rifts in South Iceland is bridged near 64°N by a zone of high seismic activity, the South Iceland Seismic Zone, which takes up the transform motion between the Reykjanes Ridge and the Eastern Volcanic Zone. The zone joins with the Reykjanes Peninsula Oblique Rift and the Western Volcanic Rift Zone in a triple junction at the Hengill Central Volcano, near 21.5°W. To the east it joins with the EVRZ near Hekla Volcano, where the deformation gradually goes spatially into magmatic mode.

The South Iceland Seismic Zone has been defined by destruction areas of historical earthquakes, Holocene surface ruptures and instrumentally determined epicenters (Figure 3). It is oriented EW, 70-80 km long and 10-15 km wide. Volcanism is insignificant in this zone, indicating that the relative movement is mostly parallel to the zone itself. Destruction areas of individual historical earthquakes (Stefánsson et al. 1993) and identified surface ruptures of individual earthquakes (Clifton and Einarsson 2005) show, however, that each event is associated with faulting on NS-striking planes, perpendicular to the main zone. The faults are expressed at the surface by N-trending arrays of NNE-striking fractures arranged en echelon. The overall left-lateral transform motion along the zone thus appears to be accommodated by right-lateral faulting on many parallel, transverse right-lateral faults (Figure 4).

Earthquakes in South Iceland tend to occur in major sequences in which most of the zone is affected. It has been argued that a complete strain release of the whole zone is accomplished in about 140 years (Stefánsson and Halldórsson 1988).

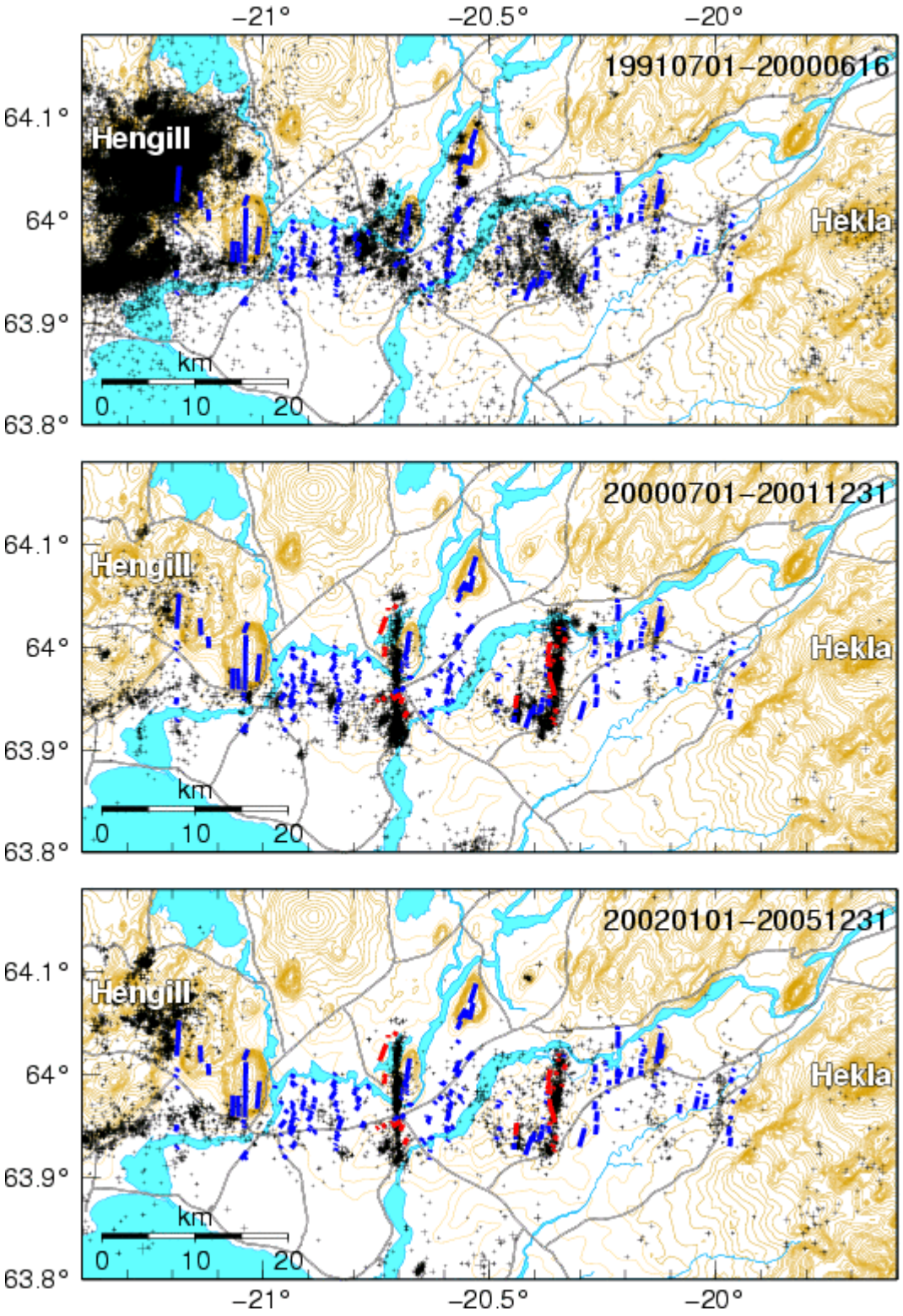

Figure 3. The SISZ between the volcanic area Hengill in west and the Hekla Volcano in the east. Blue line segments show Holocene earthquake faults, red line segments the faults of the 2000 earthquakes (Clifton and Einarsson 2005). The figure shows earthquakes from July 1991 to 16 June 2000, from July 2000 to December 2001 and from 2002 to 2005 respectively.

2.3 The Western Volcanic Rift Zone

The WVRZ branches off the main plate boundary at the Hengill triple junction and extends for about 100 km to the NE with a trend of about 30° (Figure 1). At least 3 volcanic systems have been identified within this zone but their boundaries are not clear, partly because of the glacial cover of Langjökull. They are arranged parallel to the zone itself and are side-by-side without significant en echelon arrangement. Normal faulting is very prominent in their fissure swarms, sometimes also fissuring, as dramatically demonstrated in the famous Þingvellir rift valley. Volcanic fissures are, on the other hand, not particularly common. Lava shields are very common and moderate amounts of evolved magmas have been produced in the central volcanoes.

The activity of the WVRZ appears to be quite uneven, both in time and space. Faulting of the 8000 years old lava at Þingvellir, near its southern end, indicates that as much as half the total spreading during the Holocene is occurring on this zone. This appears to die out rather quickly towards NE. GPS-measurements near the middle of the segment indicate that only 10-20% of the total spreading occurs there (LaFemina et al. 2005). No eruptive volcanic activity is known in the zone in historical times (last 1100 years), but a rifting event took place near its southern end in 1789. Significant background seismicity is detected in the WVRZ in spite of slow plate movements, particularly in its middle part.

2.4 The Eastern Volcanic Rift Zone

The EVRZ joins with the SISZ transform zone in the area of the Hekla and Torfajökull Volcanoes. From there it extends for about 120 km with a trend of about 40°, to the central area of the Iceland hotspot. Volcanic systems of this zone are arranged side-by-side and have the same trend as the zone. Apart from Hekla and Torfajökull, all the central volcanoes are located in the northern part. The southern part therefore consists of rifting structures only, mainly large eruptive fissures. Normal faults and open fissures exist but they are not prominent in the structural grain of the zone. Long crater rows and hyaloclastite ridges, the products of subglacial fissure eruptions, are the most prominent volcanic structures. Lava shields are practically absent. In this respect there is a large difference between the characteristics of the two subparallel rift zones of South Iceland.

The EVRZ has been highly active in historic time (last 1100 years). Eruptions in the size class 5-15 km^3 have occurred several times, accompanied by large-scale rifting in the fissure swarms (see e.g. Jónsson et al. 1997). The latest was the Laki eruption of 1783. No significant rifting episodes are known since the 1860's, however, in spite of considerable activity of the central volcanoes. Seismicity is abundant in the zone but it is limited to the central volcanoes in the northern part. The fissure swarms in the southern part have been seismically quiet for at least the last four decades.

2.5 The South Iceland Volcanic Zone

Volcanic activity occurs also outside the plate boundary zones in Iceland. The volcanic zone of South Iceland is of some interest here. It extends from the rift-transform junction at Torfajökull and Hekla and into the Eurasia Plate to the south. This zone is characterized by a group of central volcanoes with immature fissure swarms. This area

contains some of the most active volcanoes of Iceland, i.e. Hekla and Katla. The zone is quite active, but little or no rifting is associated with most of this activity. The earthquakes of June 2000 in the SISZ were preceded by an eruption in Hekla in February 2000 (Soosalu et al. 2005). Hekla is located at the junction of the different zones and is underlain by seismic lineations with NS trend, similar to the SISZ to the west of the volcano (Soosalu and Einarsson 1997). The interaction between the volcano and the mechanics of the seismic zone is poorly understood.

3 About seismicity in SISZ and RP

Good information on historical seismicity is available from 1700. Much less information is available before that time but still providing some insight in the nature of the crustal process of the zone and for hazard assessments in the area.

A significant feature of the SISZ earthquakes appears in Figure 4. It is based on studies of historical documents providing detailed information about the hazard and thus a basis for epicentral location, direction of fault planes and magnitudes (Halldórsson 1987; Stefánsson and Halldórsson 1988; Stefánsson et al. 1993). It is also based on detailed mapping of historical faults (Clifton and Einarsson 2005), complementing the historical information. Later work has provided the fault lengths that appear in Figure 4 (Roth 2004).

According to instrumental observations and research there is right-lateral slip on the earthquake faults as conjugative to the left-lateral motion of the SISZ. The earthquakes since year 1700 display an almost regular sequence (Figure 4) with in average 6 km distance in between. During this period the large earthquakes have not been repeated on the same faults. This already indicates that there must be a local heteorogeneity which controls where the stress is released each time. At an early stage it was stated that it was probable that such local sources were based on fluid intrusions from below the crust and that these fluids also carried along energy which contributed significantly to the moment release in earthquakes in the zone (Stefánsson and Halldórsson 1988).

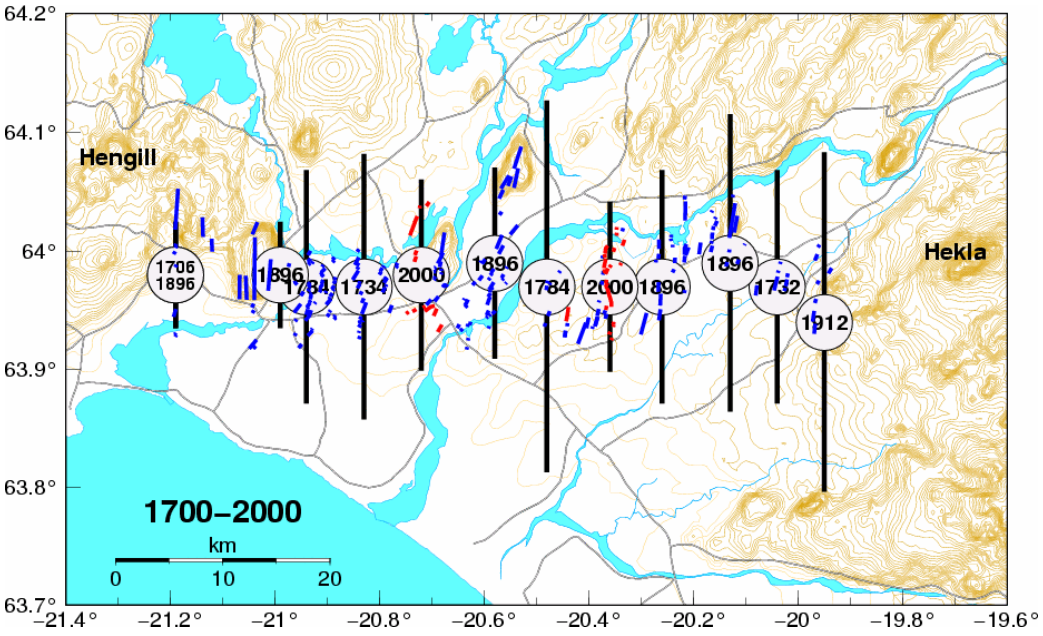

Figure 4. *Earthquakes in SISZ since 1700. The earthquakes arrange side by side each having right-lateral slip on a NS fault. The fault epicenters and magnitudes (Stefánsson et al. 1993; Einarsson et al. 2005) are estimated from historical data and the fault lengths are from Roth (2004).*

Large earthquakes (magnitude 6-7) tend to occur in major sequences in which a large part of the zone is affected. These sequences tend to last from a few days to about 3 years.

Each sequence typically begins with a large event in the central or eastern part of the zone, followed by smaller events farther west. It has been pointed out that it is to be considered that the total strain release of the zone is accomplished in around 140 years with much longer time in between individual earthquakes of a total breakthrough. The clearest example on this is the 1912 earthquake in the easternmost part of the SISZ which completed the 1896 earthquake sequence. This result is based on the historical earthquakes since 1700, on the weak information that we have of earlier earthquakes and on plate motion consideration (Stefánsson and Halldórsson 1988).

The fault lengths indicated in Figure 4 are estimated on basis of historical magnitudes. Although microearthquakes and most fissures from historical earthquakes point towards a narrow zone, i.e. only 10 km (Figure 3) the fault lengths indicated in Figure 4 point towards NS slips on faults much longer than the width of the narrow zone in many cases. Fault lengths up to 35 km are found (Roth 2004).

Intensive swarm activity occurs frequently at the western end of SISZ, Hengill volcanic area and at the eastern end, in connection with volcanic eruptions in Hekla (Figure 4). These volcanic areas are significant in relation to the strain build-up and strain release in the zone.

The two clusters of small earthquakes between Hekla and Hengill (see Figure 3 and 5) were areas of elevated seismic activity within the SISZ and probably had been there for 35 to 50 years before they proved to be in the fault area around the two magnitude 6.6 (Ms) earthquakes (Stefánsson and Guðmundsson 2006a).

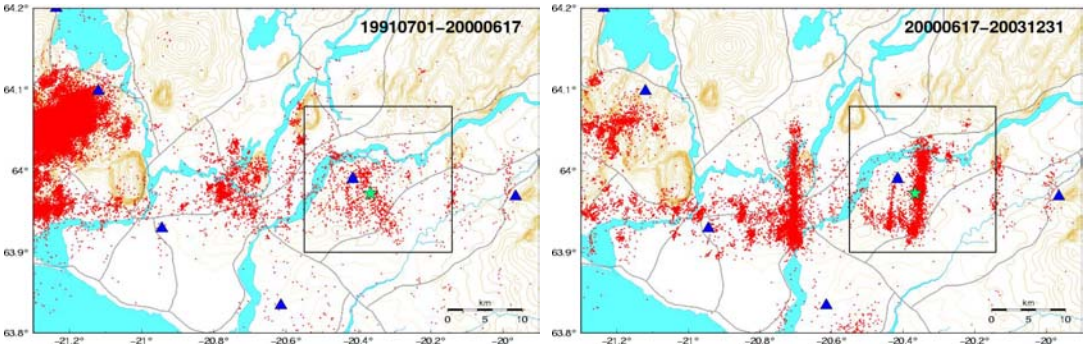

Figure 5. *Seismicity in the SISZ before (left) and after (right) the year 2000 earthquakes shown by green stars. The area of dense seismicity at the western end of the SISZ is at the junction between the SISZ and the Western Volcanic Zone, displaying high seismic activity there during a volcanotectonic episode 1994-1998. At the eastern end of the SISZ we are close to the junction of SISZ with the Eastern Volcanic Zone.*

3.1 Silence and premonitory activity before the 1912 earthquake

The large series of 1896 (Figure 4) started with the easternmost earthquake in the figure, and the whole SISZ to the west from there was apparently broken through. After this sequence the zone was seismically relatively silent for 7 years, i.e. until 1904. From that time until 1911, five earthquakes of estimated magnitude 4-4.5 (based on intensity from personal descriptions) occurred with origin in the easternmost part, i.e. well to the east of the first 1896 earthquake, and only observed by people. This would fit to emerging ideas

about premonitory processes before large earthquakes in the SISZ (see modelling chapters later in this report), i.e. a phase of starting of breakthrough from below in a medium-large earthquake, probably triggered and followed by lithostatic pressure fluid migration up into the brittle crust and gradually increasing pore pressure, finally resulting in the large earthquake. However, an observed premonitory activity of the 2000 earthquakes lasted for 30-40 years, while only 8 years before the 1912 earthquake. The premonitory activity may have started much earlier before the 1912 earthquake without being observed, and then relaxed during the 1896 sequence. Anyhow, this gives a hope for being able to record a process before a possible large earthquake in the easternmost part of the zone, possibly from the start of first partial fracturing, towards the release of the large earthquake (Stefánsson and Guðmundsson 2006a).

3.2 Microseismicity

The microseismicity, i.e distribution of small earthquakes, varies strongly with time, in intensity of course, but also spatially. Comparing right and left parts of Figure 5 provides an example of change in areal distribution of microearthquakes from before both of the large earthquakes of year 2000, towards linear distribution afterwards (Stefánsson and Guðmundsson 2005).

Figure 6 shows a cumulative number of microearthquakes in some areas of the SISZ/RP approaching the large 2000 earthquakes.

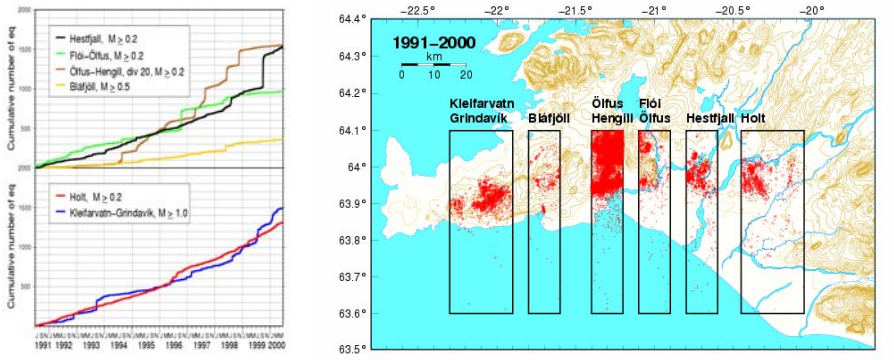

.

Figure 6. *Cumulative frequency of microearthquakes above limit of completeness, approaching the 2000 earthquakes at various sites along SISZ. They indicate stress increase in the epicenter of the first of the 2000 earthquakes (Ms=6.6), and near the western end of the active part of RP, where the dynamically triggered aftershocks occurred. The areas of study are shown to the right (Stefánsson and Guðmundsson 2006a).*

The gentle increase in number in the lower part of the figure, especially from the year 1896 implies stress increase (Stefánsson and Guðmundsson 2005; Stefánsson and Guðmundsson 2006a). It appears that during 1991-2000 relative EW motion occurred within the zone as a whole without a long-term stress build-up except at the east and the west ends of active parts of the SISZ and RP zones.

3.3 The seismicity of the Reykjanes Peninsula

As said before around year 1250 the tectonic mode in the Reykjanes Peninsula (RP) has been seismic, in contrast to a more volcanic or magmatic mode during a period 300 years before (around 950-1250). The historical documentation about seismicity of RP is less than in the SISZ. The Hengill volcanic area at the eastern end of the zone and the Krísuvík high temperature area only 25 km further west are tectonic boundaries of the eastern part of RP. The largest earthquake instrumentally recorded in the RP was within this eastern part. It occurred in 1929 and had magnitude 6.2 (Ms). In hazard assessment (based on seismic history) it is assumed that the largest earthquake here is not expected to exceed 6.5. The westernmost part of the peninsula, i.e. from Kleifarvatn to west is characterized by intensive swarm episodes, where normal faulting earthquakes are frequent. The largest magnitudes observed there are estimated around 5.5, and it is assumed probable that they will not exceed that limit.

A period of high seismic activity started on the RP just before 1900 and lasted until 1910 and again from 1915 to 1923. It is possible that these swarm sequences were triggered by the 1896 and 1912 breaking through the SISZ. An episode started with the magnitude 6.2 earthquake in 1929 and can be said to have lasted until 1935. The last intensive episode before 2000 took place from 1967 to 1973. All these episodes took to most of the peninsula.

A strong episode in the year 2000 was dynamically triggered by the earthquakes in the SISZ and took to the eastern part of RP, most intensive near the western margin of it, at Kleifarvatn, where apparently most stress had been building up before (see Chapter 3.2).

3.4 Seismic swarms migrating from the bottom of the brittle crust towards the surface

Such migration of swarms are recorded and expected in response to loading stresses on the area, and reflect upwards migration of fluids with lithostatic pressure (Stefánsson and Guðmundsson 2005; Zencher et al. 2006). They rise up to the lithostatic/hydrostatic boundary and can be applied as a measure of strain in the system and thus may provide information that has potential to estimate proximity to earthquakes in space and time. These lithostatic fluids gradually corrode the areas around the becoming earthquake fault, and cause a weekness and gradually instability which foreruns larger earthquakes.

4 Some aspects of crustal structure of the SISZ

4.1 Seismic structure

The seismic structure of the zone has been studied by active seismic (see for example Bjarnason et al. 1993; Flóvenz and Gunnarsson 1991; Tryggvason et al. 2002).

Significant results for earthquake prediction and hazard assessments were revealed in 3-dimensional velocity study, tomography, based on travel times of waves from natural earthquakes (Tryggvason et al. 2002). At a depth of 4-10 km below the Hengill area, velocity of P- and S-waves is reduced, more of the P-waves (low Vp/Vs). This is interpreted as heavily fractured volcanic fissure system and the low velocities caused by supercritical fluids, some of magmatic origin. In the SISZ itself normal velocities were found, however, with slight reduction in the Vp/Vs velocities (Tryggvason, personal communication). An increase in depth to the 6.5 km/s P-velocity is also seen from west to east along the zone, comparable to the deepening of the brittle/ductile boundary (Tryggvason et al. 2002).

4.2 The brittle/ductile boundary

The depth to the brittle/ductile boundary is a significant aspect of the structure of the seismic zone. This was studied by Stefánsson et al. (1993) which indicated depth to the ductile zone of about 6 km near the west end of SISZ and 12-13 km around the eastern part. Figure 7 is based on much longer period of data, indicating similar results although slightly deeper, 7 km at 21ºW and 13 km at 20ºW. This is not significantly different of course, especially as the depth of earthquakes is depending on strain rate as well as of stress (Stefánsson and Guðmundsson 2006a). As seen in Figure 7 there is an indication that the brittle/ductile boundary is slightly shallower to the north of the zone and slightly deeper to the south of the zone compared to inside the zone.

Deepening of earthquakes are observed near the western end of the zone (Figure 7), i.e. in the Hengill volcanic area or close to it, probably indicating high pore pressures and fast upstream of fluids below this volcanic area, rather than the bottom of the seismogenic zone.

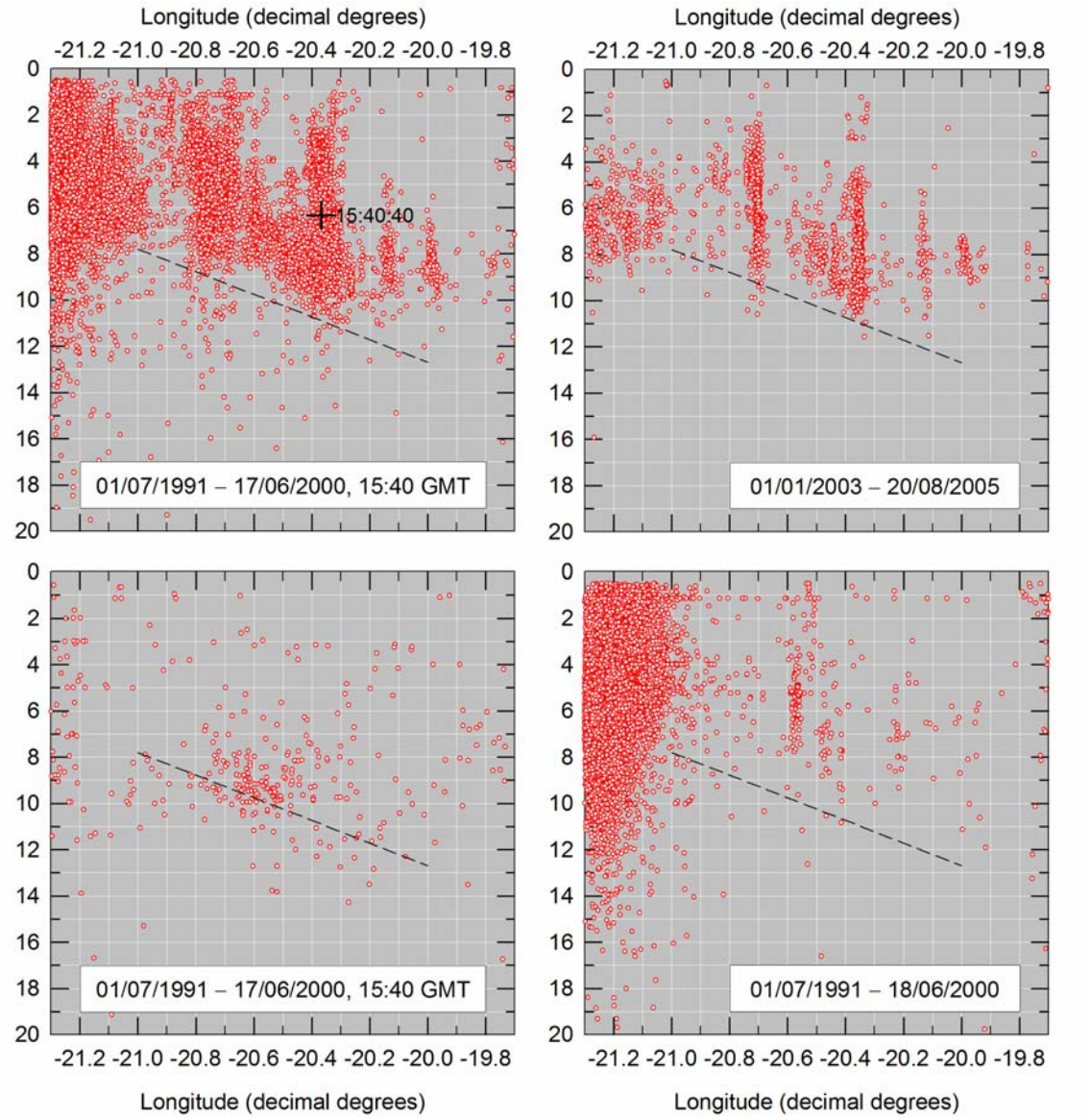

Figure 7. *The upper two figures show the depth of earthquakes inside the SISZ (63.92°-64.02°N) for a period of years before the 2000 earthquakes. The most pronounced earthquake activity is further west; i.e. in the Hengill volcano tectonic junction area releasing strong swarm activity especially in the period from 1994 to 1998, involving large tectonic strain release and volcanic intrusions at depth. The two lower figures are just south of (63.70°-63.85°N) and just to the north of (64.05°-64.20°N) the SISZ respectively.*

4.3 Low resistivity near the boundary of the brittle/ductile zone

Magnetotelluric data from several dense measuring profiles in Iceland (Beblo and Björnsson 1980; Hersir et al. 1984; Eysteinsson and Hermance 1985; Björnsson 2006) indicate low resistivity (10-20 Ohms) at depths between 10 and 20 km and even shallower in the volcanic zones. It is to be noted that this layer does not absorb seismic S-waves as should be if it would contain a large fraction of melt. It has therefore been argued that the low resistivity layer is indicating fluid mobility in a solid matrix, solid enough to transmit seismic waves (Stefánsson et al. 1996).

5 Observing crustal dynamics

5.1 Earthquake faults in the SISZ mapped by microearthquakes

Technology has been developed for mapping of active faults. Many old active faults in the SISZ and RP have been mapped in this way. Before the 2000 earthquakes seismicity in the zone was low so precise mapping by using microearthquakes was difficult. However, the large earthquakes of year 2000 triggered earthquakes of many faults that had not been seen before and can now be mapped this way, as well as others that can be more precisely mapped than before. The technology applied makes it possible to locate earthquakes with accuracy within 100 m and even below that relatively (Slunga et al. 1995). Such a mapping complemented with geological surface mapping is very valuable for modelling future earthquakes and for correct interpretation of possible premonitory signals.

Figure 8 shows microearthquakes following the large 2000 earthquakes, illuminating fault segments within the whole of SISZ (Hjaltadóttir and Vogfjörð 2005).

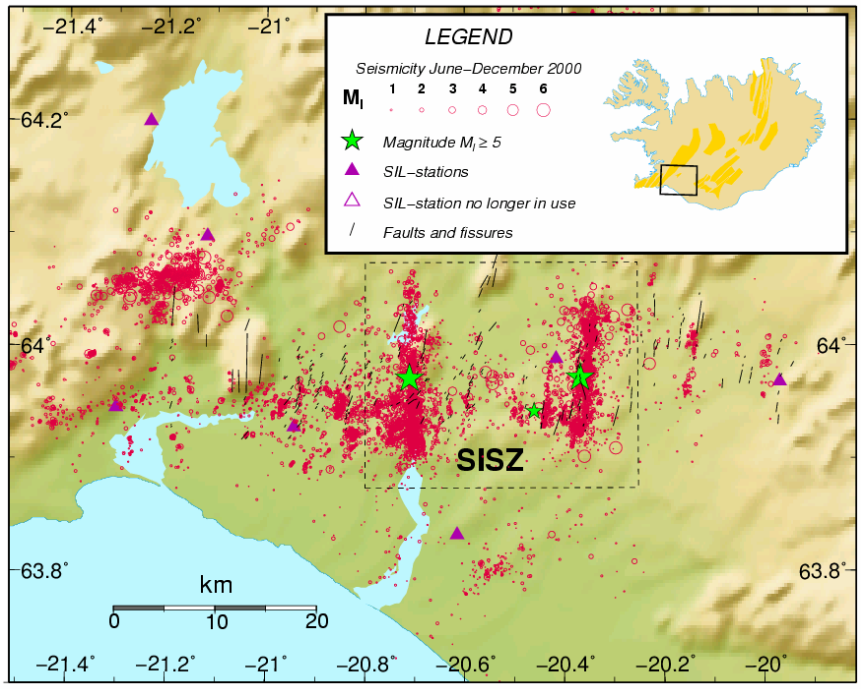

Figure 8. *The relocated aftershock activity in the SISZ between June and December 2000 shown by red circles, scaled according to magnitude. The hypocenters of the two main shocks are denoted by large green stars. The small green star shows the location of a M~5 event, which occurred 2 minutes after the June 17 event.*

5.2 *b*-values in the SISZ

Studies of *b*-values of microearthquakes in the SISZ before the two large earthquakes could identify the asperities of the earthquakes as limited areas with low *b*-values, supporting the ideas that asperities with short local recurrence times control locations of major ruptures. Mapping of *b*-values in cross sections of SISZ shows also anomalies of

high *b* at the bottom of the seismogenic crust, supporting the view of high pore fluid pressures there, and correlating with the change the thickness of the brittle crust in the middle of the SISZ (Wyss and Stefánsson 2005) (Figure 9).

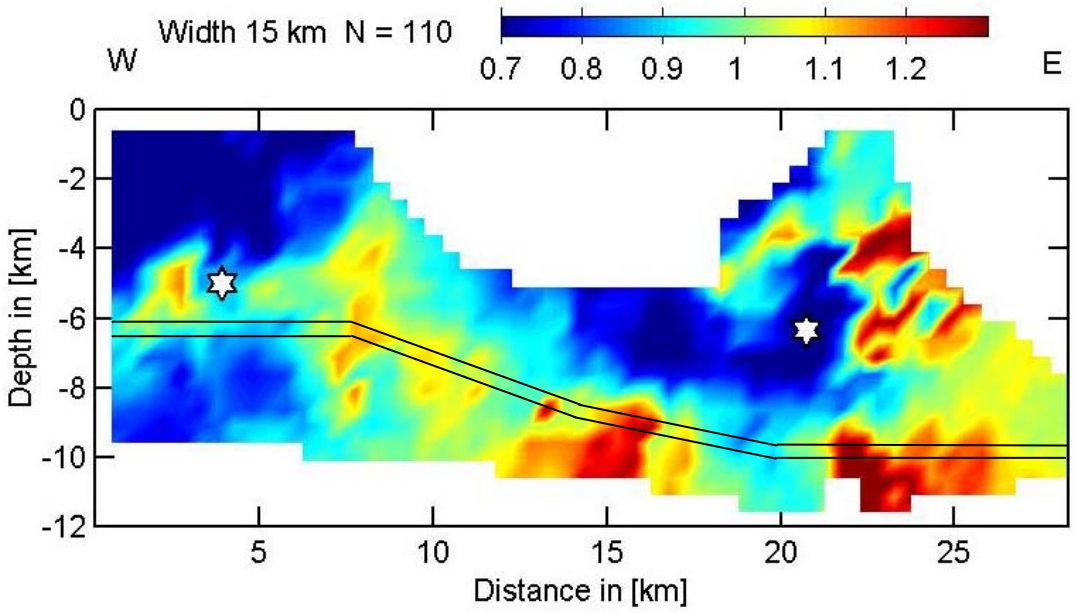

Figure 9. *Maps of b-values in cross sections (color bar) along a 15 km wide EW strip in the SISZ. The two hypocenters of the large earthquakes are marked by stars. The initial earthquake is the star farther to the east. A double line delineates the approximate bottom of the dense seismic activity. The data period is 1991-2000 (before the first large earthquake).*

5.3 Deformation studied by GPS and InSAR approaching the 2000 earthquakes

Modelling of the deformation of the SISZ area ahead of the 2000 earthquakes is mostly based on GPS campaign measurements from 1992 and onward of the area as a whole and complemented by observations by InSAR.

The crustal deformation prior to the June 2000 earthquakes is shown by a surface velocity field map of Southwest Iceland obtained from campaign and continuous GPS data collected between 1992 and 2000 (Figure 10). The pre-seismic velocity field is affected by plate spreading, inflation at Hengill and Hekla Volcanoes and subsidence at the Svartsengi geothermal area.

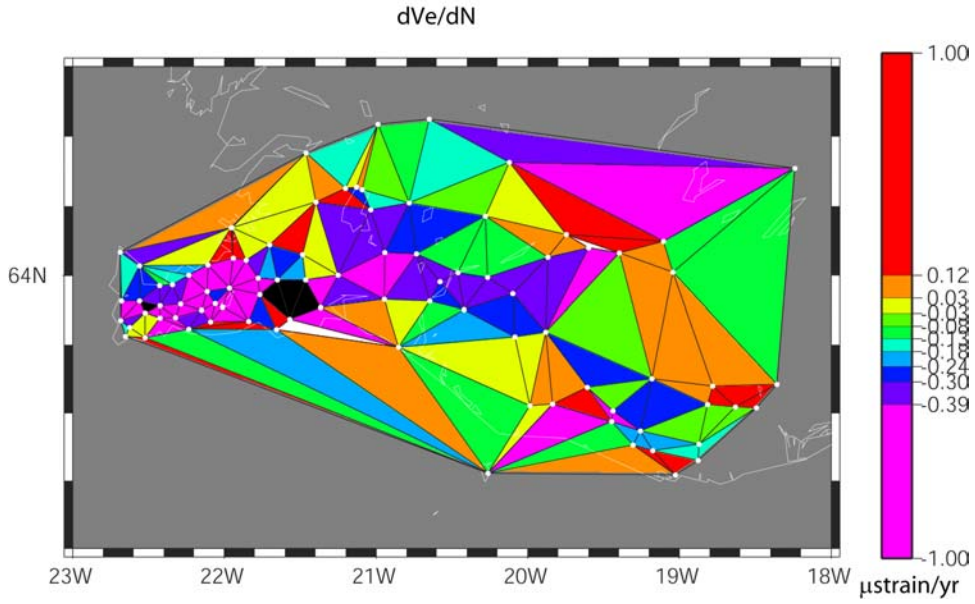

Figure 10. *Pre-seismic horizontal GPS station velocities assuming that REYK moves with a velocity of 10.5 mm/year towards west and 1.8 mm/year north (blue arrows with 95% confidence ellipses). The stars show epicentral locations of earthquakes in 1998 (white stars) and June 2000 (orange stars), and the hexagons indicate pressure sources at Svartsengi, Hengill and Hekla (Figure 6a from Árnadóttir et al. 2006).*

The velocity field shown in Figure 10 is used to calculate the strain field in South Iceland in the pre-seismic period 1992-2000. The shear strain rate is composed of several components of the gradient of the velocity field in different directions. The northward gradient of the eastward velocity component, i.e. dVe/dN, is most indicative of left-lateral motion on an EW transform, or right-lateral motion on an NS fault, as observed in the SISZ (see Figure 11). Figure 11 shows that the strain rate is high in the center of the SISZ, and decreases as we move north or south from 64°N. This pattern demonstrates that strain was concentrated in the SISZ prior to the June 2000 earthquakes. The black color around the Hengill area indicates very high negative strain rates, due to the high rate of deformation due to inflation from 1993 to 1999. The strain rates are generally high along the plate boundary on the Reykjanes Peninsula and through the SISZ, with strain rates up to about 0.5 µstrain/year.

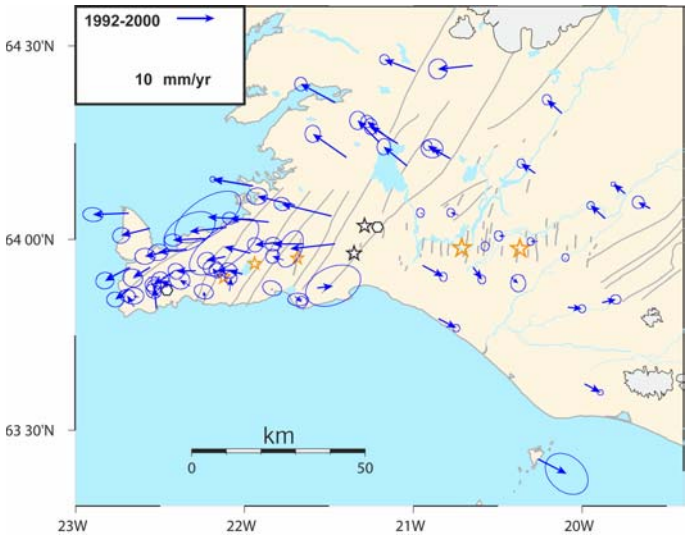

Figure 11. *The strain field during the pre-seismic period (1992-2000), shown as the northward gradient of the eastward velocity component showing left-lateral motion on EW faults, or right-lateral motion on NS faults.*

In the study of Árnadóttir et al. (2006), they first model the interseismic plate boundary deformation in Southwest Iceland assuming that it is driven by left-lateral transcurrent motion along the plate boundary, below the brittle/elastic upper crust, assuming simple screw dislocation models. This model assumes that the brittle crust is locked down to a certain depth (D) and slipping freely below with velocity (V). The velocity at the surface v is then described by Savage and Burford (1973):

$v(y) = (V/\pi) \arctan (y/D)$,

where y is the distance perpendicular to the plate boundary.

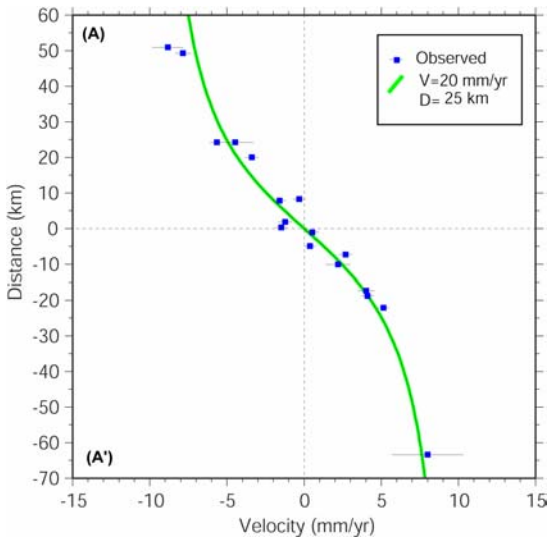

Figure 12. *GPS station velocities in the SISZ parallel to the plate boundary (blue squares) as a function of distance along a NS profile (A-A'). Results from nonlinear inversion estimating 4 model parameters (deep slip rate, locking depth, velocity shift and profile shift) are shown with solid lines. (Figure 10b from Árnadóttir et al. 2006).*

Although the pre-seismic GPS network is not dense enough to confine the width of the SISZ, Figure 12 shows that the strain rate is highest in a 20 km wide strip along the SISZ. This observation is to be compared to the concentration of microearthquakes and length of mapped NS faults within a 10-15 km wide zone in the SISZ. But also to be compared with the up to 30 km fault lengths in individual earthquakes in the zone (see Figure 4), which suggests that the assumption of a 10-15 km wide zone may be a simplification, i.e. that another mode of earthquake release may exist, which takes to a broader zone, within a longer time span of occurrence.

Next, Árnadóttir et al. (2006) generate more complex model to explain the pre-seismic GPS velocity field. Their preferred plate boundary kinematic model is a 3D dislocation and point source model with left-lateral slip along the plate boundary on the Reykjanes Peninsula and below the SISZ, and opening across the Western and Eastern Volcanic Zones (Figure 13). The model parameters cannot be uniquely determined from the GPS data. In particular, there is a trade-off between the locking depth and the deep slip rate. For constant deep slip rates in the range 16-20 mm/year, they find a 5-7 km locking depth on the Reykjanes Peninsula, and 8-11 km depth below the SISZ. These locking depths show reasonable agreement with the thickness of the seismogenic layer in Southwest Iceland, which appears to vary between 8 and 10 km.

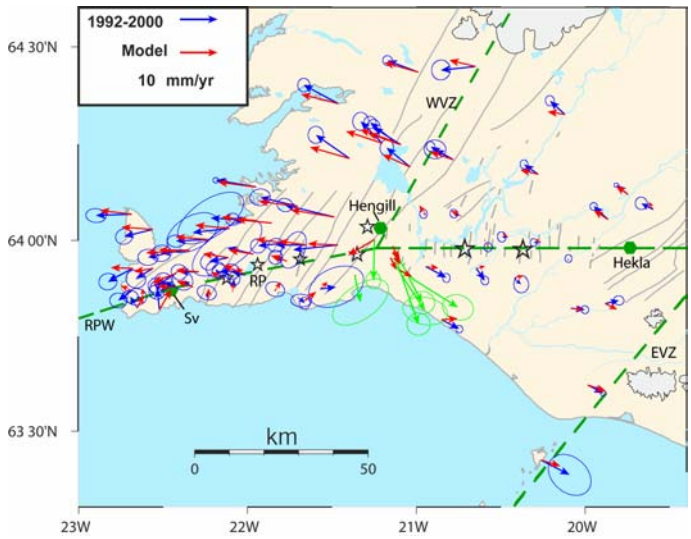

Figure 13. *Observed horizontal velocities (blue arrows) and predicted velocities (red) from the preferred 3D dislocation and point source model. The green lines show the surface projections of the dislocations (RP: Reykjanes Peninsula; WVZ: Western Volcanic Zone; EVZ: Eastern Volcanic Zone). The hexagons show the point sources (Sv: Svartsengi; Hengill and Hekla) (Figure 12a from Árnadóttir et al. 2006).*

Using the preferred plate boundary model from Árnadóttir et al. (2006) we can estimate the rate of Coulomb failure stress change during the pre-seismic time interval, using standard methods (e.g. Harris 1998). Figure 14 shows that the inflation in Hengill and left-lateral slip below 7 km depth along the plate boundary on Reykjanes Peninsula combine to increase the Coulomb failure stress on NS, right-lateral strike-slip faults on the Reykjanes Peninsula, such as ruptured in the triggered earthquakes on June 17, 2000. The Hengill inflation appears to have acted to decrease the Coulomb failure stress on NS faults east of Hengill. This is in accordance with the reduction of shallow earthquakes in

this same area during the Hengill inflation (Stefánsson and Guðmundsson 2006a). It may also explain why the June 2000 earthquake sequence did not progress further west following the June 21, 2000 main shock.

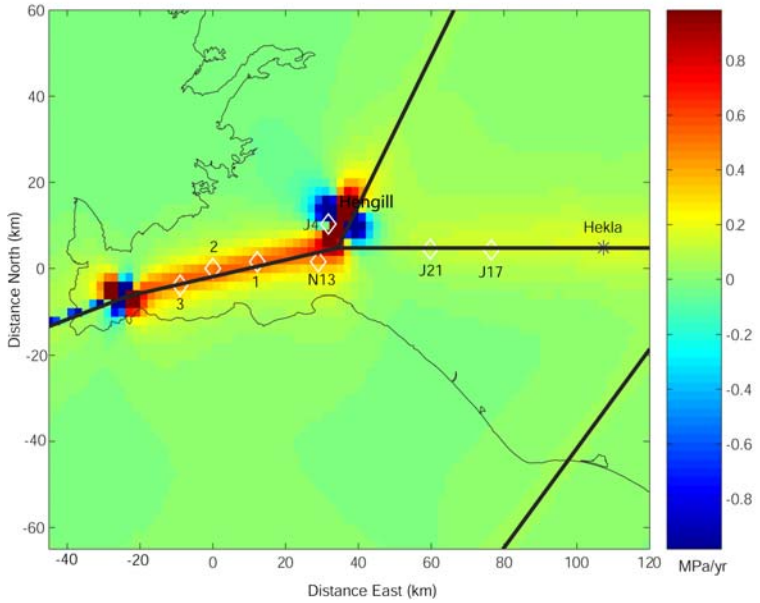

Figure 14. *The rate of Coulomb failure stress change at 5 km depth, on NS right-lateral strike-slip faults, caused by plate boundary deformation. The diamonds denote earthquake locations, where the June 17 and 21 main shocks are labelled J17 and J21 respectively, the numbers 1, 2, 3 refer to the June 17 triggered earthquakes. The M=5 1998 earthquakes in the Hengill and Ölfus are labelled J4 (June 4, 1998) and N13 (November 13, 1998). Warm colors (yellow to red) indicate an increase in Coulomb failure stress. Small changes in Coulomb failure stress (0.001 MPa) have been shown to correlate with areas of increased seismicity following a mainshock (e.g. Harris 1998).*

The post-seismic deformation in the SISZ following the June 2000 main shocks during the time interval from 2000 to 2004 can be explained by either viscoelastic relaxation of the lower crust and upper mantle in response to the coseismic stress changes or afterslip at 8-14 km depth (Árnadóttir et al. 2005). The optimal viscoelastic models have lower crustal viscosities of about 0.5-1x10^{19} Pa*s and a less well constrained upper mantle viscosity about 3x10^{18} Pa*s.

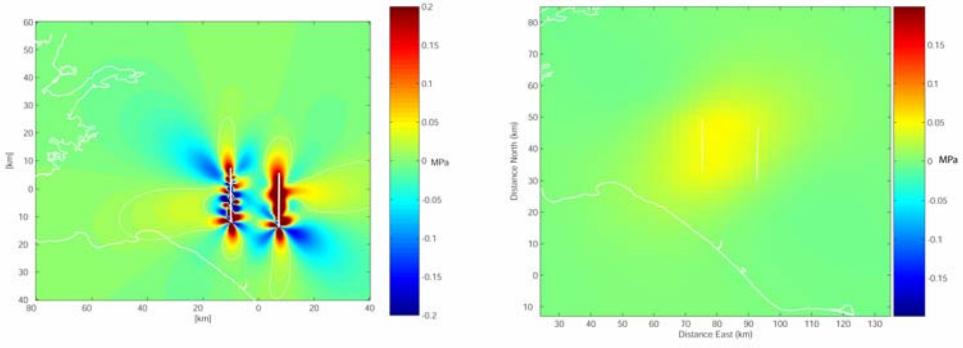

Figure 15. *Coulomb failure stress change due to afterslip (left) or viscoelastic relaxation (right) from 2000 to 2004, assuming NS dextral receiver faults, calculated at 5 km depth.*

The total geodetic moment of the two Mw=6.5 June 2000 earthquakes has been estimated as $1x10^{19}$ Nm (Pedersen et al. 2003) using Mo=μ, where μ is the shear modulus, A is the fault area, and u is the mean slip. Sigmundsson et al. (1995) used the rate of geometric moment, Mo/μ, as a measure to compare the rate of moment build-up in the SISZ due to plate spreading, estimated as 1.0-2.5x$10^7$$m^3$/year, to the rate of seismic moment release in historical times, estimated as 2.0-2.3x$10^7$$m^3$/year (Stefánsson and Halldórsson 1988; Hackman et al. 1990). The geometric moment of the two June 2000 main shocks is about 3x$10^8$$m^3$ whereas the moment built up since the Ms=7.0 earthquake in 1912 is 9-22x$10^8$$m^3$ (Pedersen et al. 2003). The June 2000 main shocks therefore released at most only one-third of the moment built up due to plate spreading in the previous 88 years. Árnadóttir et al. (2005) estimate that their afterslip model adds about 1x$10^8$$m^3$, over the 4 years following the earthquakes. Based on this, it is concluded that there is still a significant amount of moment stored in the brittle crust in the SISZ, suggesting that large earthquakes are likely to occur in the SISZ in the near future. Based on Coulomb failure stress calculations (Figure 15) they conclude that the areas of large co-seismic stress increase east of the June 17 and west of the June 21 ruptures, continue to be loaded by the post-seismic deformation.

5.4 Estimation of the general rock stress tensor in the area

The rock stress tensor in the area has mainly been estimated from fault plane solutions of microearthquakes and also surface fault slip data.

Angelier et al. (2004) studied the average stress tensor by inversions of microearthquake fault plane solutions in the period 1991-1999 and in an area covering 63°-64.5°N and 18°-22°W. A major σ1 axis is found 52 east of north (near horizontal). An opposite stress regime is found for a smaller part of the data, i.e. with σ1 perpendicular, 140° east of north.

In Angelier et al. (2006) the average stress tensor for the SISZ area, i.e. the area 20.0º-21.6ºW longitude and 63.85º-64.15ºN latitude has been studied by inversion of microearthquakes for the period 1991-2005. For the main average stress tensor field over the area, the σ1 azimuth is 41°-47ºNE and the σ3 is 131°-137ºSE. This field takes to 70% of the 34000 microearthquakes used.

5.5 Local stress permutations

A secondary stress field is also found explaining 30% of the data, which is approximately opposite in directions, i.e. σ1 134º-137º and σ3 41º-47º, σ2 is approximately vertical. The conclusion of the authors is that the primary stress field is in excellent agreement with the left-lateral transform motion along the EW direction. A permutation, however, occurs between the σ1 and σ3 axis causing the secondary stress field. A study of the location of the earthquakes expressing these two stress fields shows that they are intimately connected in space and time, in many cases down to the scales of days and hundred meters, which "suggests that the elastic rebound and stress drop as well as migration of fluids following earthquakes play a major role to induce systematic permutation between extreme principal stresses" as the authors say.

5.6 Local stress anomalies near the June 21 earthquake

As reported in WP5.6 of the PREPARED Third Periodic Report a special study was carried out on the spatial differences in revealed stress directions from microearthquakes near the fault of the second earthquake, i.e. June 21. The periods selected are 1999 to June 17, 2000, June 17 to June 21, 2000 and June 21 to end of year 2000. Significant evolution of stress axes directions are seen along the NS strike of the fault but also with depth (see Figure 16). These results show a modification of the state of stress in the southwestern part of the Hestfjall Fault occurring after the earthquake of June 21, 2000 and a larger deviation of the stress at 5 to 10 km depth, i.e. ~40° deviation, instead of ~20° deviation at 0-5 km depth.

0-5 km		Az.	Pl.
Before	σ_1	43	4
	σ_3	132	8
During	σ_1	50	5
	σ_3	138	13
After	σ_1	23	2
	σ_3	113	7

5-10 km		Az.	Pl.
Before	σ_1	52	6
	σ_3	144	12
During	σ_1	45	18
	σ_3	130	13
After	σ_1	12	19
	σ_3	105	7

Figure 16. *Stress tensor inversion for the southwestern part of the Hestfjall Fault. Three periods of time are considered (before, during and after the seismic crisis) and the two different depths (between 0-5 km in the table situated on the left, and between 5-10 km in the table on the right). We realize the stress tensor inversion for the southwestern part of the Hestfjall Fault.*

The observed spatial deviation of stress with depth is attributed by the authors to an effect of the pore or fluid pressures beneath five kilometres depth or to rheological contrasts.

In WP5.6 of the PREPARED Third Periodic Report are also studied the fault slips on the surface in similar area as above (Bergerat and Angelier 2005). The results are in general the same as in the inversion of microearthquakes. Minor fields seen are explained by stress permutations, dyke injections and partly by decoupling. Relatively more normal faulting is seen in the geological slip data results than in the seismological results, expressing the time difference of the observations, i.e. reflecting the evolution from rifting to transform motion during the last 2-3 million years.

5.7 Stress variations with time in the SISZ

Variations of stresses in time and according to regions were studied in WP2.4 of the PREPARED Third Periodic Report and to some degree more local variations. Following information is provided there about stresses in three areas of the SISZ, related to three areas of earthquakes in the zone.

Following areas were defined around three notable earthquakes in the studied time period:

- The Ölfus November 1998 earthquake, latitude 63.9° to 63.99°N, longitude 21.47° to 21.0° W.
- The June 17, 2000 earthquake (J17), latitude 63.9° to 64.05°N, longitude 20.5° to 21.25°W.
- The June 21, 2000 earthquake (J21), latitude 63.88° to 64.07°N, longitude 20.9° to 21.63°W.

In these areas we divided the seismicity into three temporal intervals, 1991 to 1995, 1996 to June 17, 2000 (the first M=6.5 event) and June 17, 2000 to 2003, and inverted the focal mechanisms for the stress field. The results for the maximum principal stress axis and the maximum horizontal stress are:

J17 area:

1991-1995 σ1	N51°E	plunge	30	SH	N52°E
1996-2000	N54°E		20		N54°E
2000-2003	N58°E		20		N57°E

J21 area:

1991-1995 σ1	N50°E	plunge	5	SH	N51°E
1996-2000	N43°E		20		N44°E
2000-2003	N34°E		35		N31°E

Ölfus area:

1991-1995 σ1	N37°E	plunge	45	SH	N37°E
1996-2000	N35°E		30		N36°E
2000-2003	N28°E		30		N28°E

The authors conclude that the average stress direction is very stable in the case of the June 17 area. In Lund et al. (2005) a large scale inversion is made of all events in the June 17 area, which shows that the average direction of SH, the horizontal compressions component of the stress is N53°E. Studying changes in time and space it is revealed that during 1991-1995 the direction of horizontal component is stable around N50°E but 1996-2000 (before earthquake) is more varied, indicating some change in 1996. In 1996 there is a clear although moderate increase in the rate of earthquakes as indicated in Stefánsson and Guðmundsson (2005), indicating stress increase.

In the June 21 area there appears to be a northward rotation of the maximum stress. In the case of the two first time periods, the authors of WP2.4 of the PREPARED Third Periodic Report point out that the difference is well within the confidence limits. For the aftershocks, as we will see below, there are indications that there are inhomogeneities in the stress field which causes the apparent rotation of the average stress northwards.

In the Ölfus area, stress directions are rather stable all through the observed time periods. It is, however, observed that the Ölfus area, which is located west of the core SIL area, has a more north-southerly direction of the maximum stress.

5.8 The relevance of stress estimations for assessment of potential future earthquakes in the SISZ

The questions that are raised in connection with earthquake prediction research are of course relevant if stress directions can tell us something about stress build-up ahead of an earthquake. Probably in what appears here they do not say much. The variances in stress directions before the earthquakes are too large, i.e. the small variations that are observed are within confidence limits according to the last chapter. There are, however, indications for northward rotation of maximum stress (near horizontal) before the June 21 earthquake and a more definite rotation to north expressed in the aftershock period. Both for the June 17 and the June 21 earthquakes the local stress ($\sigma 1$) long time ahead (1991-1995) of the earthquakes is 50°-51°NE. Coming closer in time to the earthquakes (1996-2000) the stress in June 17 area has rotated to east to 54°NE, but in the June 21 area it has rotated northward. i.e. to 43°NE. After the earthquakes the stress in the June 17 area has still rotated to east to 58°NE, but in the June 21 area the stress has rotated north to 34°NE.

If we compare the observations above with the general stress direction for the area 41°-47°NE revealed from Angelier et al. (2006), it is indicated that in the June 17 area the eastward angle was larger than average, and increasingly so from 1991 (the beginning of the dataset) until the release of the large earthquake. This coincides with stress increase as indicated by the release of microearthquakes in the same area (Stefánsson and Guðmundsson 2006a). In the same report it is also indicated that stress increases are moderate as they are evened out by by the release of fluid-driven earthquakes migrating towards the surface.

Although the indicated stress changes ahead of the earthquakes are within confidence limits they are in agreement with what would be expected considering that the SISZ plate motion is locally hampered by the June 17 asperity.

It is plausible that continuous, general westward plate motion along the SISZ would cause stress increase complying with eastward rotation of the compressional stress in the June 17 area if the motion is hampered by a stopping asperity there. It may therefore be considered if the eastward rotation of stress after the June 17, 2000 earthquake may be an indication that the stress release in the June 17 earthquake was far from being complete for that region and that stress is increased in a nearby region.

The situation would be quite different for the June 21 earthquake area. It did not have stress increase ahead of the earthquake, according to the microearthquakes, being in the stress shadow of the 17 June earthquake, and the stress direction goes down to 43°NE approaching the time of the earthquakes, i.e. the plate motion is not building up stresses there. After the earthquakes the direction is still more northward (N34°E) in this place, i.e. coming closer to what would be if the plate motion had no effect, which can be expected to be due north in this "weak zone", i.e. the June 21 area is still in a stress shadow for the general plate motion.

The data here are of course not strong indicator for the conclusions above. However, in the light of that only a fraction of the stored strain in SISZ was released in the 2000 earthquakes this indication cannot be neglected. The question is if an earthquake releasing much of the leftover a strain energy will occur slightly to the west of the June 17 earthquake fault.

5.9 Local stress estimations near the June 17 earthquake

Local scale estimations studied by Lund et al. (2005) show that in the area of the first large earthquake, June 17, the stress state in the lower part of the crust is different from the upper part in the period from 1996 to just before the initial large earthquake. In this period the earthquakes deeper than 7.5 km show great variations in the maximum horizontal stress (Figure 17). It is inferred also that at 7.5 km depth there is a transition from predominantly strike-slip at shallow depths to another stress regime below, possibly indicating more normal faulting. Studying horizontal compressions with time from 1991 to 2000 in the depth range below 7.5 km have high standard deviations, suggesting high-level of heteorogeneity, making stress inversions unsecure. However, the horizontal compressions show large spatial variations as seen in Figure 17. These variations in standard deviations and apparent horizontal compressions seem to persist from 1996 until the release of the 2000 earthquakes.

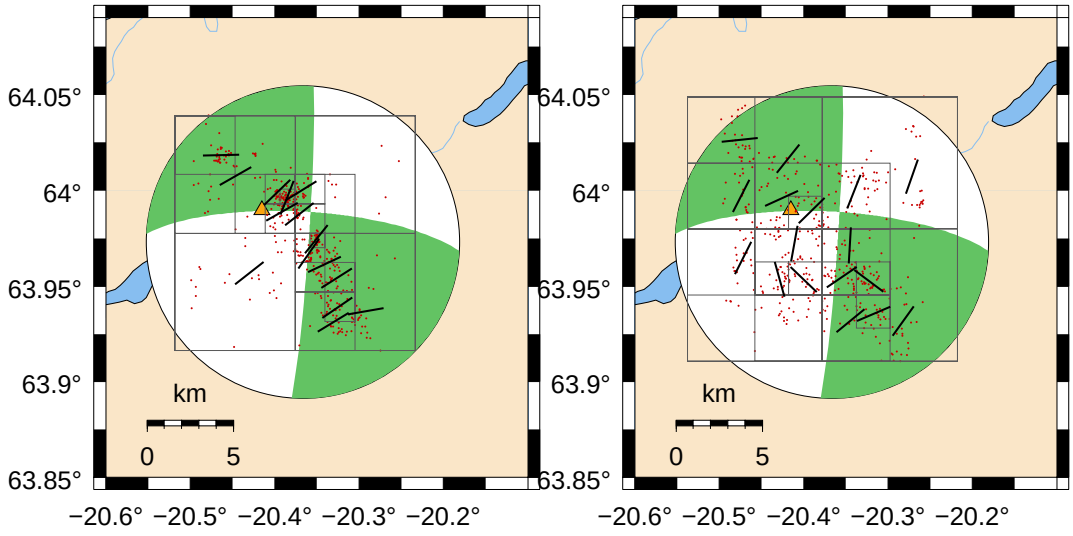

Figure 17. *Epicentral region of the June 17, 2000, M=6.5 earthquake. The focal mechanism is for the large event, from the Harvard database but centered on the SIL location. The red dots are earthquakes from the SIL catalogue from January 1996 to June 17, 2000. The squares show the partitioning of the events using the quadtree algorithm. The black lines are the directions of the maximum horizontal stress, i.e. above 7.5 km (left figure) and below 7.5 km (right figure).*

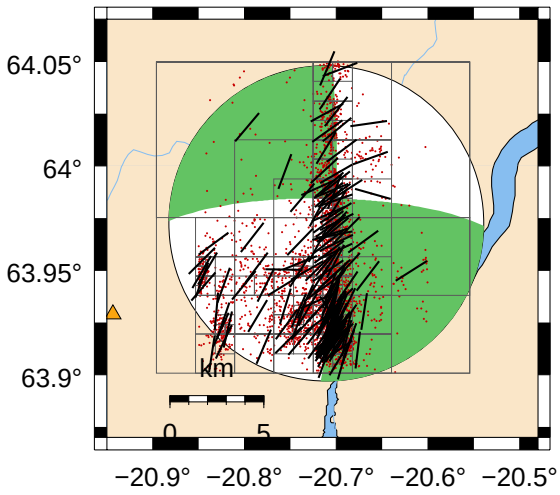

Figure 18. *Epicentral region of the June 21, 2000, M=6.5 earthquake. The focal mechanism is for the large event from the Harvard database but centered on the SIL location. The red dots are earthquakes from the SIL catalogue from June 17, 2000 to June 17, 2001. The squares show the partitioning of the events using the quadtree algorithm. The black lines are the directions of the maximum horizontal stress.*

In the earthquake on June 21 there are no such depth variations as observed in WP2.4 (Figure 18). In the aftershocks there are interesting variations in the horizontal maximum stress east of the nothern part of the fault, where EW compressions are observed. This may reflect stress build-up by fluid intrusion into the northern part of the June 21 fault or in a fracture system to the east near by the fault, i.e. between the the June 17 and the June 21 faults.

In studying the local stress heteorogeneity it is a preliminary conclusion in WP2.4 that possible candidates for the heteorogenous stress state in the lower part of the seismogenic crust include fluid intrusions, magmatic intrusion, structural heteorogeneity or combination thereof.

5.10 About the stress inversions in general

The stress directions inferred above in WP5.6 and WP2.4 are in general agreement. The selection of areas and time periods of study cause some differences when going to regional and local scales. Heteorogeneities across a weak zone, as the SISZ is, must be considered. Significant local differences can be expected from within the zone, to near its border and to farther away from it. A common result of the studies is large stress variations with depth, explained by fluid activity or some other rheological heteorogeneity. The change of this observed heterogeneity with time in some of these studies, especially in WP5.6 study, strongly point towards fluid mobility as a cause for the strong local variations. The conclusion in WP2.4 about change of stress domain at 7.5 km depth in the area of the first earthquake is also in agreement with fluid mobility at greater depth penetrating upwards. In this area the seismic/ductile transition is at 11 km depth (see Chapter 4.2).

The heteorogeneity of the stress estimations express fluid/rock heteorogeneity and mobility of hydrostatic fluids. It is in agreement with the dual mechanism model of Stefánsson and Halldórsson (1988) which describes local interplay in time and space between plate motion and intrusions. In WP6.2 it is shown by earth-realistic models that high pore fluid pressures can efficiently migrate from below the brittle/ductile transition to shallower depths if a pressure-dependent permeability model is assumed, in which fluid overpressure opens small hydraulic fractures (Zencher et al. 2006). In the earth-quake warning parameter EQWA (WP3.1) high lithostatic pressures are assumed up to a depth of 3.5 km. This assumed knowledge is basis for absolute stress estimations. The success of estimating stresses by this method is an indirect approach to demonstrate the existence of high pressure lithostatic fluids at shallow depths in the crust and thus supports the assumption that high fluid pressures migrate upwards in the crust in response to strain changes.

It is concluded that one of the approaches to monitor crustal processes leading to large earthquakes is analysis of detailed stress variations in space and time and detailed modelling to explain these changes. Mobile fluids in the crust certainly cause heterogeneity in stress estimations from microearthquakes and in a way break down the methods usually applied in stress estimations. However, as these heterogeneities are time and space dependent in an observable way they have a potential for observing in time and space a process approaching fracturing conditions. It is significant to develop new methods, independent of the assumed conditions requested for stress inversions, to observe these changes better by directly applying microearthquake information like location and fault plane solutions.

6 Description of multidisciplinary premonitory observations in approaching the 2000 earthquakes

Various types of premonitory observations in approaching the 2000 earthquakes have been described in the PREPARED Third Periodic Report, especially WP2 and WP3 (see also Stefánsson and Guðmundsson 2005; Stefánsson and Guðmundsson 2006a). In modelling the SISZ processes we must also take such processes into account.

6.1 Premonitory seismic activity

Various seismic information based on locations and fault plane solutions in approaching the 2000 earthquakes are described in Stefánsson and Guðmundsson (2005) and Stefánsson and Guðmundsson (2006a). One of these descriptions appears in Figures 19, 20 and 21. Figures 19 and 20 describe positions of microearthquakes in the area 10 weeks prior to the first large earthquake and show that the locations of microeathquakes start to move fast up and down, south and north, along the fault direction, 1-2 weeks before the earthquake. It starts at 11 km depth and near the northern end. This is explained in such a way that two weeks before the first large earthquake motion started along a large part of the fault plane. The motion is hampered a day before the earthquake by the hard core asperity, which is gradually fractured in earthquakes concentrated there, mostly during the last day before the earthquake. A simple algorithm to visualize this motion is shown in Figure 21, which simply accumulates the distances between consecutive microearthquakes on weekly basis after each new microearthquake, i.e. at each earthquake point we see from the abscissa how much earthquakes have been moved along the fault plane during one week before it. Selecting a day for the plot would make the "long-term precursor" weaker but the asperity nucleation precursor stronger.

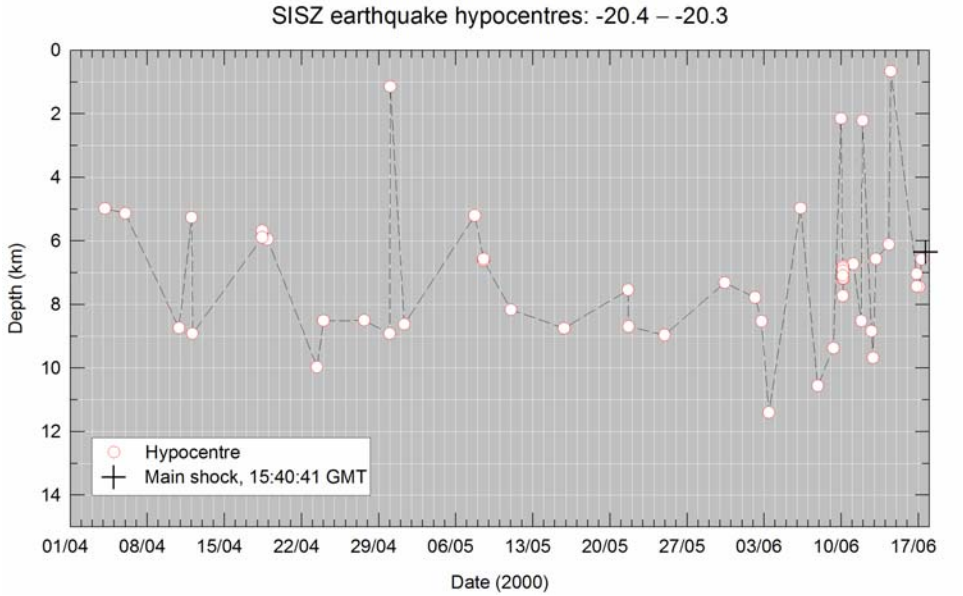

Figure 19. *Depths of microearthquakes (down to magnitude -1) with time from April 1, 2000 until the June 2000 earthquakes.*

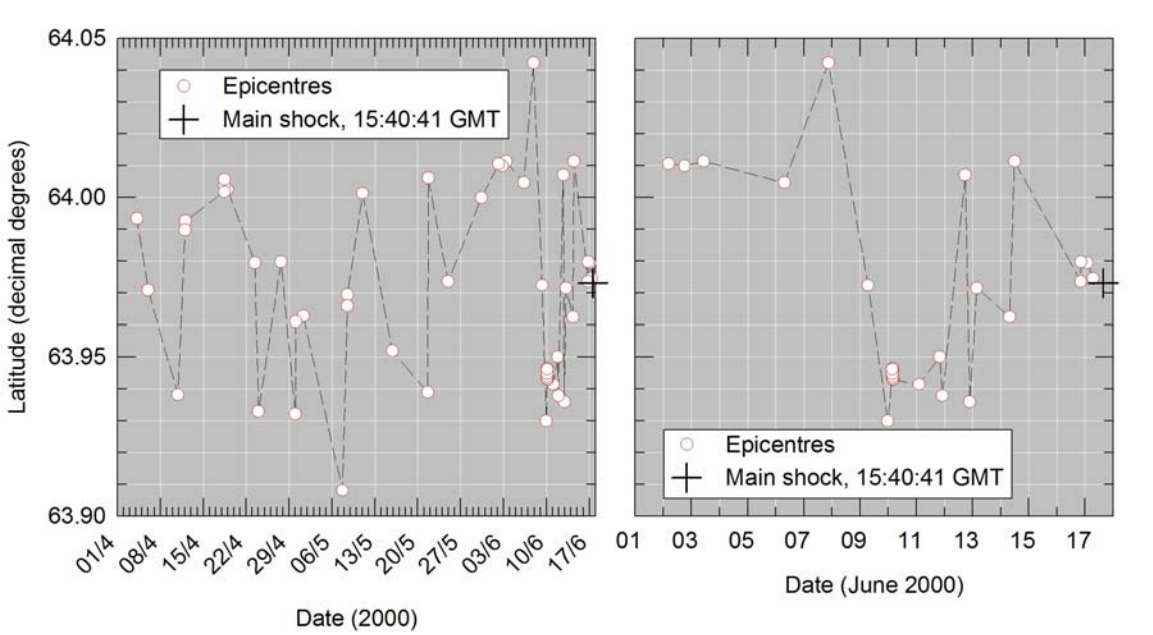

Figure 20. *Epicenters of microearthquakes along a horizontal strip along the NS elongated fault plane of the first 2000 earthquake during with time before the June 17 earthquake.*

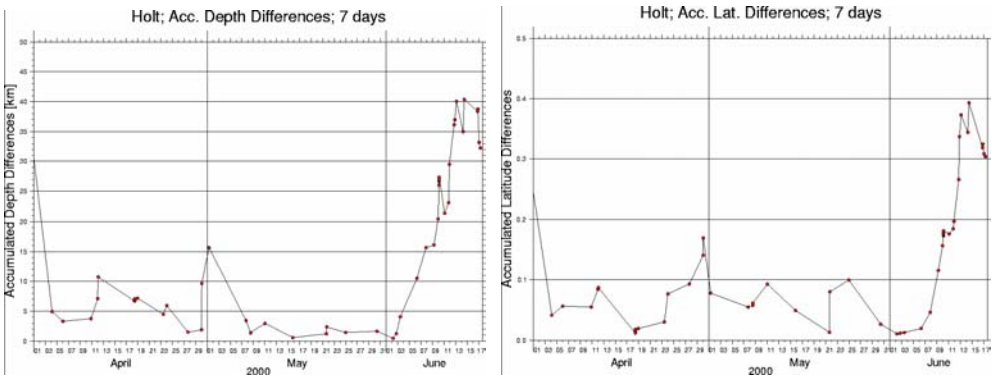

Figure 21. A*ccumulated distances between consecutive microearthquakes with time. A week is selected as a coincidence period. The figure to the left shows accumulated depths, while the figure to the right shows distance changes along the fault, i.e. latitudes.*

These results are not shown here to demonstrate that we have found the final algorithm to make a short-term prediction. We have simply seen a preprocess to an earthquake which starts at the bottom of the seismogenic crust. It remains to see by statistical study in what way it can be used in warning procedures. How often have such events happened before?

6.2 A new short-term seismic warning algorithm

In WP3.1 of the PREPARED Third Periodic Report a warning algorithm is described which basically is aiming towards finding an earthquake asperity and trying to alert for if the probability of breaking the alert comes to a certain limit (see also Slunga 2003; Stefánsson and Guðmundsson 2006b).

The components of the EQWP algorithm are based on stress level estimates, based on location and fault plane solutions and assumptions on rheological properties and that the earthquakes release by fluids with lithostatic pressures. It is also based on microearthquakes "1/b" (representing toughness) fault radius and activity rate of microearthquakes. In hindsight good results are obtained in this approach to find the place of an asperity and to find when it is near breaking strength.

6.3 An evidence for the June 17 asperity

The existence of a central asperity is shown directly and indirectly in different kinds of observations. Plotting aftershocks shows a core 3 km in height at around 6 km depth, interpreted as an asperity (Stefánsson et al. 2003; Hjaltadóttir and Vogfjörð 2005). The time function of the break-up of the asperity is also observed by strainmeters in the area, in the first part of the earthquake record (Figure 22).

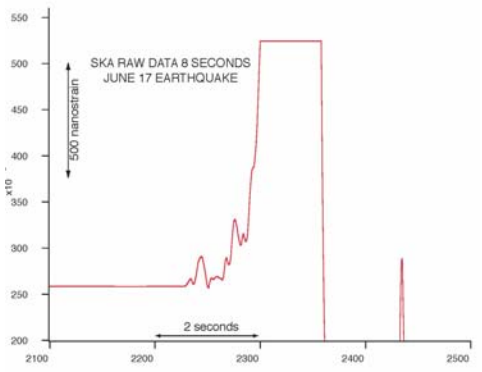

Figure 22. A *strainmeter record from SKA 20 km to the west of the June 17 earthquake. A nucleation phase is shown 1.8 seconds before motions starts on the fault plane as a whole.*

6.4 Stress increase and stress relaxation before the earthquakes from shear-wave splitting

The shear-wave splitting studies described in WP2.5 of the PREPARED Third Periodic Report and in Stefánsson and Guðmundsson (2006b) show a gentle increase in shear-wave splitting time during 5 months before the first earthquake, implying stress increase at seismic stations in the zone. Interesting for modelling is that they show stress

relaxation during the last weeks before the earthquake, coinciding with the start of the earthquake process and stress/fluids reorganization seemingly starting at this time.

6.5 Information from radon measurements

Results of radon evaluations are described in WP3.2 of the PREPARED Third Periodic Report and also in a short overview in Stefánsson and Guðmundsson (2006b). The most significant finding is high correlation of radon anomalies during 1999-2001 over the entire SISZ. The stations show very similar fluctuations in the concentration of radon. This points to one origin. And even if this origin has not yet been found or defined this shows that the earthquakes are a part of a large-scale process and that this process started long time before the earthquakes.

6.6 Is the SISZ a weak zone?

With the average maximum horizontal stress driving the motion across the SISZ around 45º from the direction of motion, the SISZ would be defined a weak fault, i.e. weaker probably both in effective rigidity and incompressibility than its surroundings. Fluids with lithostatic pressure penetrating the crust from below tend to expand all fractures which they penetrate. The weakness should also cause relatively high compressional stress component perpendicular to the boundary between the weak zone and the adjoining stronger crust. This tendency would be strongest just near the boundary and can lead to local NS fractures there in response to fluids penetrating upwards from below. This can be a part of the physical explanation of the NS direction of the earthquake faults perpendicular to the EW general fault motion. This would also be generally in accordance with an expansion across the zone in addition to the transfom motion as postulated by the oblique direction of the SISZ to the plate motion direction.

But what are the direct evidences for such a weakness of the fault?

- High density of earthquake fractures within a 10 km wide EW zone.
- Concentration of microearthquakes within a 10 km wide zone.
- The strain observations and modelling studied by GPS of this report point to highest strain rate in a 20 km wide strip along the SISZ.
- There is an indication for a weak velocity anomaly, i.e. lower velocities along the zone than outside (Tryggvason et al. 2002; Ari Tryggvason, personal communication).

7 Modelling of the SISZ

7.1 Modelling earthquake probability changes due to stress transfer

Modelling work has been carried out to apply the historical earthquake catalogue since 1700 to try to estimate in hindsight the site and time of the next earthquake (Roth 2004; Richwalski and Roth 2006; WP6.1 in the PREPARED Third Periodic Report) in the SISZ. The idea was to see if earthquakes occur at times when high stress has built up and at place of highest stress or at places with Coulomb stress changes above 0.01 MPa. It could be shown (Árnadóttir et al. 2003) that the first large earthquake of June 17, 2000 could have triggered the second earthquake on a parallel fault plane, 20 km away from the June 21 event, assuming a homogenous half space model. This created certain optimism that it might be possible to use the historical catalogue of the SISZ to better understand such relationships.

Mixed elastic and inelastic half-space model was applied. A viscoelastic-gravitational extension was applied to model post-seismic creep process (the parameters applied are given in the PREPARED Final Report).

Temporal variations of shear stress were calculated estimating the contribution of each of the historical earthquakes, the plate tectonic stress changes as well as post-seismic stress relaxation. Both, elastic and viscoelastic model responses, were calculated. Also Coulomb stress changes were calculated to see if Coulomb stress would better predict the earthquakes than shear stress analysis.

The result of this modelling did not lead to definite conclusions about the time and location of the next event. On basis of the model assumed, it turned out to be impossible to constrain the stress field such that the impending event would occur at its known location. There are mostly large areas in which stress levels showed to be high enough to trigger an event.

By restricting the possible site to the known epicenter of the earthquake it was studied at what stress level the earthquake would occur there. The result was that regarding absolute shear stress levels the maximum expected stress before an earthquake was only reached in 50% of the cases. Regarding the Coulomb stress levels, the result was not much better. Short-term clustered events are triggered at sites when the Coulomb stress is above the named threshold. In the long-term, the probability of foreseeing the earthquakes is the same as in the shear stress case.

The authors of this study conclude that strong events in the SISZ are presumably not triggered by preceding events (Richwalski and Roth 2006; WP6.1 in the PREPARED Third Periodic Report).

7.2 Modelling stress in the solid matrix of the SISZ and pressure fluids permeating it

This has been carried out in WP6.2. The following aspects have been addressed employing theoretical crack models:

- Modelling of fault complexities in the SISZ employing crack models in layered elastic media (Bonafede and Ferrari 2005). These models show that the fault surface should bend at layer interfaces in order to release local stress drop values prescribed by fault rheological laws. Offsets and discontinuities of surface breaks observed in the field may be explained in this way.

- Lithosphere-asthenosphere interaction under the SISZ, taking into account viscoelastic constitutive relationships and intrusive events across rheological discontinuities (Rivalta and Bonafede 2005). These models show that an interface between an elastic and a viscoelastic layer develops high deviatoric stress when a tensile crack, characterized by uniform overpressure, crosses it. The overpressure may be provided by fluids released by underlying magma. The model may be applied to understand the sharp concentration of low magnitude seismicity at the brittle/ductile transition in the SISZ.

- Fault instability in the SISZ, taking into account poroelastic constitutive relationships and pressure-dependent permeability (Zencher and Bonafede 2005; Zencher et al. 2006).

- Triggered seismicity and the interaction between the two large earthquakes of year 2000 (Antonioli et al. 2006).

An innovative outcome of this modelling, which is significant for explaining various observations in the SISZ, is that high pore pressure values can efficiently migrate from below the brittle/ductile transition to shallower depths if a pressure-dependent permeability model is assumed, in which fluid overpressure opens small hydraulic fractures. Poroelastic parameters for basaltic rocks were computed from experimental data assuming different intrinsic permeabilities (from 10^{-15} to $10^{-20}m^2$). The effect of pressure-dependent permeability is important for rocks characterized by lower intrinsic permeability ($<10^{-17}m^2$), while practically no effect is found in rocks with higher intrinsic permeability ($>10^{-16}m^2$), as shown in Figure 23. These solutions show that episodes of fluid migration can increase the pore pressure up to lithostatic values and then decrease substantially the instability threshold of a fault region, with obvious seismogenic implications (Zencher et al. 2006).

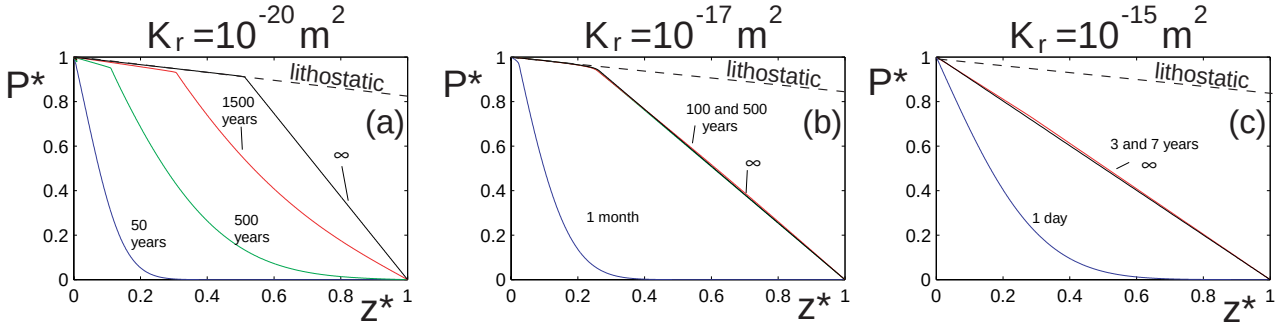

Figure 23. *Theoretical modelling in thermo-poroelastic media with pressure-dependent permeability, related to the opening of small hydrofractures, shows that rocks with low intrinsic permeability K_r propagate slowly but efficiently near-lithostatic pressures upward from the brittle/ductile transition (z*=0). Non-dimensional units are employed for pore pressure P* and vertical coordinate z*.*

This modelling can explain various of the observations mentioned and shortly described in this report like low Vp/Vs ratio and time-dependent seismic tomography, low resistivity at seismogenic depths, radon anomalies, high *b*-values near the bottom of the seismogenic crust, migration of foreshocks before the June 2000 earthquakes, and especially in the nucleation (several days) phase of the earthquake.

In general, these modelling results can explain the local source effects which control the place of an earthquake in the SISZ. In particular, they can explain why earthquakes have not been repeated at the same fault since year 1700 but rather they arrange site by site, along the whole SISZ, with an average inter-distance of 6 km in-between the faults. The most nearby explanation is that fluids migrate as pores from the upper mantle into the lower crust on a time-scale much longer than the time between main earthquakes. They migrate into the elastic crust in response to strain loading. They modify the fracturing conditions around a becoming fault to be released in due time by an earthquake at the same time as the tectonic strain. After a major earthquake, breaking up to the surface, deep fluids probably become exhausted or, in any case, the fault region has attained higher permeability, possibly greater than $10^{-16}m^2$, the critical value for pressure dependent permeability, which is not favourable for upflow of pore fluids from below. In both cases high pore pressures cannot be reached again in the fault region for a long time. The next time when we have reached high strain, another place has developed more favourable conditions for pore fluids from below to migrate into the brittle crust.

The long-term prediction of the site of the 2000 earthquakes was based on the general idea of seismic gaps, i.e. that it is most probable that an earthquake will occur in the zone, where there is a lack of release during known history since 1700. It was also based on the tentative suggestion that small earthquakes that had been persistent in these gaps for at least a decade before the 2000 earthquakes had to do with intrusion of magmatic fluids from below. The present modelling and the reported observations which it can explain puts a profound theoretical basis behind these intuitive ideas, which were the basis for warnings more than 10 years before the 2000 earthquakes.

7.3 Long distance triggering of earthquakes

Among the most spectacular observations after the 2000 earthquakes was the triggering of a number of medium-large earthquakes up to distances of 100 km along the SISZ. In particular three events were detected in the first minute after the June 17 earthquake (Vogfjörð 2003) within 90 km distance from its epicenter. The origin time of these events correlates with the arrival time of seismic waves generated by the June 17 mainshock, as they swept westward, suggesting a causative link between them and the mainshock. The temporal evolution of dynamic stresses generated by the mainshock at the hypocenters of these three early events was modelled, assuming a four layer structure and an extended fault for the mainshock. All the three events were found to occur before the assessment of the static stress level in their hypocenter location, this kind of effect is then defined as "instantaneous" dynamic triggering. Such a kind of dataset is rather exceptional since waves from triggered events are superposed to the mainshock. Direct modelling of the temporal response of a fault to the stress perturbations caused by the mainshock was performed assuming a rate-and-state dependent fault rheology, which could explain a wide temporal spectrum of triggering effects (Figure 24). In previous studies this kind of fault constitutive law was shown to be consistent with instantaneous triggering effects provided that quite large stress perturbations are considered, that are not suitable in the far field. A condition for instantaneous triggering in the far field was here found as high pore pressure in the fault regions of the triggered events. For the smallest event here analyzed occurred 8 seconds after the mainshock without a well-constrained focal mechanism, the observed trigger effect could be reproduced assuming a right-lateral fault with a N25°E strike. For the other two events with larger magnitude that occurred 26 seconds and 30 seconds after the mainshock in the Reykjanes Peninsula, NS right-lateral faults were assumed, in agreement with geological observations. A paper (Antonioli et al. 2005) has been accepted by *J. Geophys. Res*.

Crustal structure	Depth range (m)	Vp (m/s)	Vs(m/s)
	0-1100	3200	1810
	1100-3100	4500	2540
	3100-7800	6220	3520
	>7800	6750	3800
Mainshock parameters	Bilateral rupture, rise time 1.6 seconds, strike 7°, dip 86°, rake 180°, fault dimension from aftershock distribution, slip distribution from geodetic data inversion (Pedersen et al. 2003)		
R&S friction parameters	μ_*=0.7, a=3 10^{-3}, b=10^{-2}, L=1 mm, α_{DL}=0.3		
Tectonic forcing	V_o=2cm/year		
Perturbed faults parameters	Fault dimension ~10 km, recurrence time ~10-100 years		

Figure 24. *Description of the rheological properties of the region as they have been assumed in various types of modellings.*

7.4 Some basic properties underlying the dynamics of the SISZ

In various chapters of this report are described significant features or models of the dynamics of the SISZ, which are a basis for understanding the dynamics of the zone.

An innovative outcome of the modelling work within PREPARED is that high pore pressure values can efficiently migrate from below the brittle/ductile transition to shallower parts of the crust. This modelling is based on earth-realistic parameters for the area and supported by and can explain various observations and other modellings in the SISZ (WP6.2 of the PREPARED Third Periodic Report; Zencher et al. 2006).

A general feature of the SISZ is stable motion at depth and corresponding stable build-up of strain in a 10-15 km broad EW zone in the upper brittle part of the crust. This EW zone is a weak zone compared to the surrrounding crust to north and south, penetrated from below by fluids with high pressures. The shearing strain in the zone is a result of continuous EW plate motion and intermittently loaded by the nearby volcanic activity and the activity of the adjacent rifts and hotspot/plume. The zone has a NS expansion complying with the difference between the general direction of the plate motion in the area and the direction of the plate boundary and complying with its weakness.

Interaction between tectonic motion along the SISZ and intrusion of fluids from below which change the pore fluid pressures on a long- and short-time scale is a significant feature of the zone. This was tentatively described in Stefánsson and Halldórsson (1988) and in Stefánsson (1999). Thus two processes control the release of earthquakes in the zone, the fluid inflow from below, which seems to be significant in controlling where earthquakes are released each time in a dense fault fabric (with less than 6 km spacing and according to *b*-value studies possibly down to 2 km spacing) and the plate motion which controls largely the strain that is released each time in earthquakes. The time for build-up of pore fluid pressures at each location to be enough for triggering large earthquakes seems to be much longer at each place than the 140 years interval postulated between total stress release in the zone.

7.5 The release of earthquakes/the earthquake cycle

Not counting all information here the following stages of an earthquake cycle is postulated, based on Stefánsson and Guðmundsson (2005) and Stefánsson and Guðmundsson (2006a) and the modelling efforts described in this report.

Ongoing all the time is stable motion at depth. Fluids are continuously, slowly released from the ductile deeper part of the crust, near the brittle/ductile boundary.

The stable motion is disturbed at times with earthquakes, unstable process:

Step 1) An old fault is (mostly) seismically dormant for a few to several hundred years. It was near totally released in an earthquake a few hundred years ago, both as concerns tectonic shearing as well as pore pressures.

Step 2) After some time, time length both based on the strain rate and availability fluids, fluids carrying lithostatic pressures start to penetrate up into the damage zone of the

brittle crust as cracks open, carrying high fluid pressures from below and gradually creating higher pore pressures at shallow depths in the crust. Medium-size earthquakes occur at some parts of the fault, but the slip does not proceed along the whole fault while stress around the fault is heterogeneous. The fault as a whole is not ready to slip. It creates volumes in the crust where minor seismic swarms are frequent, related to the upstream of the fluids, assumed to be mostly water. The heteorogeneity of the fault area opens the gates for local upflow of fluids, and the local stress conditions are modified by fluid/rock corrosion and strain around the fault. Gradually the fault is corroded by the fluids to such a degree that an asperity is left which the fluids pass by. The existence of the strong core heterogeneity controls locally the crustal response to the regional strain.

Figure 25 is a schematic description of some observed features before the June 17 earthquake in a 10*10 km area around the fault.

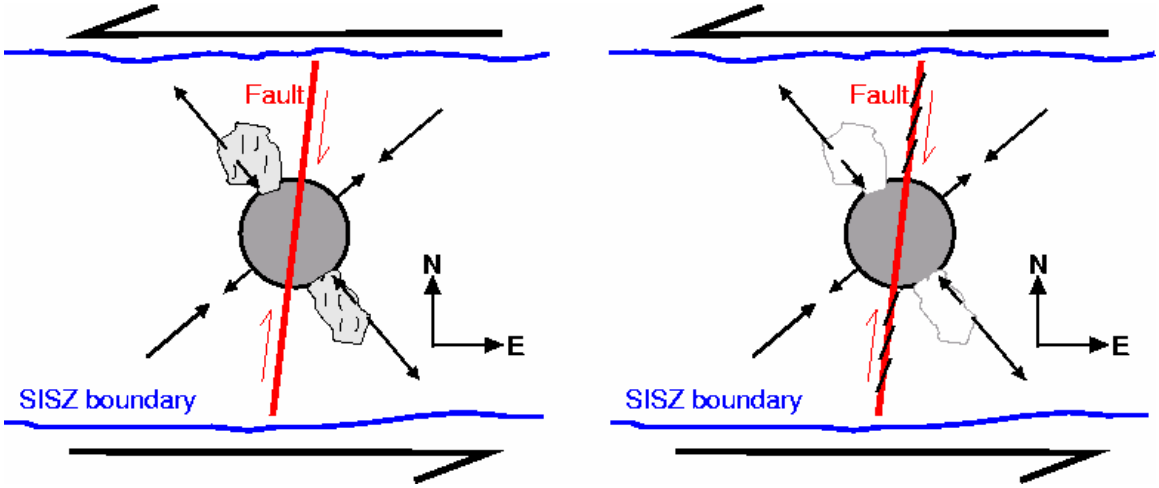

Figure 25. *Schematic picture of the conditions around the June 17 earthquake before its occurrence in the framework of the SISZ. The EW motion across the SISZ is shown by left-lateral arrows, and the boundaries of the 10 km SISZ is shown with blue lines. The June 17 fault (red) has a strike of 7ºNE. The 3 km diameter asperity is shown in dark grey. The regional horizontal stress axes are shown by arrows, and the maximum horizontal compression is here taken as 50ºNE. The local field heterogeneity caused by the left-lateral steady motion across the hard core is indicated by opposite short arrows. The areas of the premonitory swarm activity for decades, the "dilavolume" is in light grey (left figure). The line segments indicate frequent fault planes. The right figure describes the last 17 days before the earthquake. The microearthquakes now cluster near the fault plane and mostly below 6 km, with fault planes en echelon in accordance with the right-lateral motion which has started at depth (Stefánsson and Guðmundsson 2006a).*

Step 3) Initiation at depth of fault movement along an old NS fault, accompanied and pushed by fluids streaming into the fault. The fluids causing overpressures in the swarm activity volumes (dilavolumes) shift to the fault area, which has a better direction to release the plate motion strain. The fault motion, which starts down in the ductile part, and the normal faulting part between say 7-13 km propagates horizontally along the fault plane and gradually also upwards, as well as fluids which help to lower the normal pressure on the fault. A weakness in the fault finally shows up by accelerated motion of

the fault plane as a whole, shown by small earthquakes all over the fault area, and gradually by small but high stress earthquakes from an asperity, a hard core, which gradually is broken in response to the fault motion. In this way the relative stability in the fault system is broken down and unstable fault motion of the earthquake starts (Stefánsson and Guðmundsson 2006a).

Step 4) The release of plate motion strain and of fluid pressures in the epicentral area is complete, so the only earthquakes left are microearthquaes close to the fault. The fluids in the fault area have shifted place towards the earthquake fault and fluid pores near the earthquake fault fracture migrate to the fault because of the local stress changes caused by the fracturing. Long-time aftershock activity persists along the fault because of pore pressure in response to small everyday stress changes.

It is indicated that the place of an earthquake is controlled by the time for the build-up of fluids in individual fault damage zones while the size of the earthquake is depending on when it occurs within the 140 year cycle. The build-up time for enough fluid amount for triggering a large earthquake seems to be a few hundred years, may be of the order of 300 years. This is indicated already in Figure 1, if the two 2000 earthquakes are skipped. These earthquakes were relatively small, being also early in the 140 years cycle (Halldórsson and Stefánsson 2006). Some older data seem to indicate the same. These indications are extremely significant if proven to be right, and must be studied better.

8 About warnings/predictions of future earthquakes in the SISZ

The estimation made soon after the 2000 earthquakes (Stefánsson et al. 2003; Árnadóttir et al. 2005) that possibly only ¼ of the moment build-up in the SISZ was relased in the 2000 earthquakes has not been significantly changed as a result of this study. It was suggested that most part of this moment was stored in the easternmost part, and to a smaller degree in the western part of the zone, where no significant earthquakes took place.

It is, however, a question if a significant part of the moment build-up near both ends of the zone were released by recent tectonic activity in the Hekla Volcano especially the last 35 years and the Hengill area during the volcano-tectonic episode 1994-1998. This should be studied further.

In light of the small size of the two 2000 earthquakes and the long time since the large (magnitude 7.1) 1784 earthquake occurred, the possibility of a repetiton of a large earthquake in that area should not be neglected.

There are no as clear signs now of an impending large earthquake in the SISZ/RP zones as were before the 2000 earthquakes in SISZ. They were signalled by earthquake gaps and persistent seismicity for a long time.

The hope of detecting an impending earthquake before it strikes lies in detecting a preparatoty process on a long- and a short-term by studying stress increase in a large area by various sensors, and at last a strain relocation process where fluid mobility is involved.

The activity of lithostatic fluids in the earthquake build-up process provides hopes that the next large earthquake fault can be identified well before it strikes. Observable steps as described above must be detected and studied to have a hope for long- and short-term warnings on intensity and time.

Observations of microearthquake activity have been the most significant to detect the fault, the strong asperity and nucleation process of large earthquakes. The significance of fluid migration at the base of the brittle crust in the earthquake nucleation process has been modelled and observed in this project. This is significant for future forecasts of at least some large earthquakes. The problem of earthquake forecast and prediction may be by this brought to a solution by monitoring observable fluid processes and fluid/rock interaction. This signifies the use of as small earthquakes as is possible to detect down at the brittle/ductile boundary. This signifies that a special microseismic system for detecting earthquakes down to -1 or -2 at the base of the crust should be operated at suspect faults in addition to regular networks going down to magnitude 0. Even smaller events should be studied, by listening to acoustic tremors for example by acoustic sensores in deep boreholes.

Concentrations of watching in the SISZ during the next years should be in the easternmost part of the SISZ, i.e. around 20ºW and 21.1ºW, although no clear signs show up there so far of a large earthquake preparation. The area around 20.5ºW should not be neglected either. The reasons are that the two 2000 earthquakes possibly did not release

the whole potential for earthquake release there. Microseismic activity between the two 2000 earthquakes has not yet disappeared.

Although much earthquake strain was triggered on the Reykjanes Peninsula after the 2000 earthquakes, large areas known for earthquakes with magnitudes 6-6.5 are probably stress loaded, i.e. a 20 km area west of the Hengill volcanic area and the westernmost part of the Reykjanes Peninsula.

9. Acknowledgements

This work is a part of the project PREPARED (EVG1–CT–2002–00073) funded by the European Commission.

References

Angelier, J., R. Slunga, F. Bergerat, R. Stefánsson & C. Homberg 2004. Perturbation of stress and oceanic rift extension across transform faults shown by earthquake focal mechanisms in Iceland. *Earth. Plan. Sci. Lett*. 219, 271-284.

Angelier, J., F. Bergerat & R. Stefánsson 2006. Seismotectonics of the newly formed transform zone near a hot spot: earthquake mechanism and regional stress in the South Iceland Seismic Zone. *J. Geophys. Res.*, submitted.

Antonioli, A., M.E. Belardinelli, A. Bizzarri, & K.S. Vogfjörð 2006. Evidences of dynamic triggering during the seismic sequence of year 2000 in South Iceland. *J. Geophys. Res.*, accepted.

Árnadóttir, Þ., S. Jónsson, R. Pedersen & G.B. Guðmundsson 2003. Coulomb stress changes in the South Iceland Seismic Zone due to two large earthquakes in June 2000. *Geophys. Res. Lett.* 30(5), 9(1-4).

Árnadóttir, Þ., S. Jónsson, F.F. Pollitz, W. Jiang & K.L. Feigl 2005. Postseismic deformation following the June 2000 earthquake sequence in the South Iceland Seismic Zone. *J. Geophys. Res.* 110(B12), 12308, 1-13.

Árnadóttir, Þ., W. Jiang, K.L. Feigl, H. Geirsson & E. Sturkell 2006. Kinematic models of plate boundary deformation in Southwest Iceland derived from GPS observations. *J. Geophys. Res*, submitted.

Beblo, M. & A. Björnsson 1980. A model of the electrical resisitivity beneath NE-Iceland, correlation with temperature. *J. Geophys*. 47, 184-190.

Bergerat, F. & J. Angelier 2005. Pliocene-Holocene tectonics of the oceanic transform fault zone revealed by brittle tectonic analysis in the South Iceland Seismic Zone. In: Abstracts of the EGU General Assembly, Vienna, Austria, April 24-29, 2005.

Bjarnason, I.Þ., W. Menke, Ó.G. Flóvenz & D. Caress 1993. Tomographic image of the mid-Atlantic plate boundary in Southwestern Iceland. *J. Geophys. Res*. 98, 6607-6622.

Björnsson, A. 2006. Temperature of the Icelandic crust: Inferred from electrical conductivity, temperature surface gradient and maximum depth of earthquakes. *Tectonophysics*, accepted.

Bonafede, M. & C. Ferrari 2005. Complexities of strike-slip faults in the SISZ interpreted in terms of material heterogeneities. In: Abstracts of the EGU General Assembly, Vienna, Austria, April 24-29, 2005.

Clifton, A. & P. Einarsson 2005. Styles of surface rupture accompanying the June 17 and June 21 earthquakes in the South Iceland Seismic Zone. *Tectonophysics* 396, 141-159.

DeMets, C., R.G. Gordon, D.F. Argus & S. Stein 1990. Current plate motions. *Geophys. J. Int.* 101, 425-478.

DeMets, C., R.G. Gordon, D.F. Argus & S. Stein 1994. Effect of recent revisions to the geomagnetic reversal time scale on estimates of current plate motions. *Geophys. Res. Lett.* 21, 2191-2194.

Einarsson, P. 1991. Earthquakes and present-day tectonism in Iceland. *Tectonophysics* 189, 261-279.

Einarsson, P., M. Khodayar, A. Clifton, B. Ófeigsson, S. Þorbjarnardóttir, B. Einarsson & Á.R. Hjartardóttir 2005. A map of Holocene fault structures in the South Iceland Seismic Zone. In: Abstracts of the EGU General Assembly, Vienna, Austria, April 24-29, 2005.

Eysteinsson, H. & J.F. Hermance 1985. Magnetotelluric measurements across the eastern volcanic zone in South Iceland, *J. Geophys. Res*. 87, 10093-10103.

Flóvenz, Ó.G. & K. Gunnarsson 1991. Seismic crustal structure in Iceland and surrounding area. *Tectonophysics* 189, 1-17.

Geirsson, H., Þ. Árnadóttir, C. Völksen, W. Jiang, E. Sturkell, T. Villemin, P. Einarsson, F. Sigmundsson & R. Stefánsson 2006. Current plate movements across the mid-Atlantic Ridge determined from 5 years of continuous GPS measurements in Iceland. *J. Geophys. Res.*, accepted.

Hackman, M.C., G.C.P. King & R. Bilham 1990. The mechanics of the South Iceland seismic zone. *J. Geophys. Res.* 95, 17339-17351.

Halldórsson, P. 1987. Seismicity and seismic hazard in Iceland. In: D. Mayer-Rosa, J.M. van Gils & H. Stiller (editors), Activity Report 1984-1986 and Proceedings of the XX ESC General Assembly, Kiel, Germany, 1986. *Publication Series of the Swiss Seismological Service* 101. European Seismological Commission, 104-115.

Halldórsson, P. & R. Stefánsson 2006. Reevaluation of historical earthquakes. *Veðurstofa Íslands - Greinargerð.* Icelandic Meteorological Office, Report, in press.

Harris, R.A. 1998. Introduction to special section: Stress triggers, stress shadows, and implications for seismic hazard. *J. Geophys. Res.* 103, 24347-24358.

Hersir, G.P., A. Björnsson & L.B. Pedersen 1984. Magnetotelluric survey across the active spreading zone in Southwest Iceland. *J. Volc. Geotherm. Res*. 20, 253-265.

Hjaltadóttir, S. & K.S. Vogfjörð 2005. Subsurface fault mapping in Southwest Iceland by relative location of aftershocks of the June 2000 earthquakes. *Rit Veðurstofu Íslands* 21, Icelandic Meteorological Office, Research Report, 18 pp.

Jónsson, S., P. Einarsson & F. Sigmundsson 1997. Extension across a divergent plate boundary, the Eastern Volcanic Rift Zone, South Iceland, 1967-1994, observed with GPS and electronic distance measurements. *J. Geophys. Res.* 102, 11913-11930.

Khodayar, M. & P. Einarsson 2002. Strike-slip faulting, normal faulting, and lateral dike injections along a single fault: Field example of the Gljúfurá fault near a Tertiary oblique rift − transform zone, Borgarfjörður, West Iceland. *J. Geophys. Res*. 107(B5), ETG 5-18.

Kristjánsson, L. & G. Jónsson 1998. Aeromagnetic results and the presence of an extinct rift zone in western Iceland. *J. Geodynamics* 25, 99-108.

LaFemina, P.C., T.H. Dixon, R. Malservisi, Þ. Árnadóttir, E. Sturkell, F. Sigmundsson & P. Einarsson 2005. Geodetic GPS-measurements in South Iceland: Strain accumulation and partitioning in a propagating ridge system. *J. Geophys. Res*. 110(B11), B11405, 1-21.

Lund, B., M. Arvidsson, R. Böðvarsson & R. Slunga 2006. Crustal stress anomaly before the M=6.5 17 June 2000 earthquake in South Iceland. *Geophys. Res. Lett.*, submitted..

Pedersen, R., S. Jónsson, Þ. Árnadóttir, F. Sigmundsson & K.L. Feigl 2003. Fault slip distribution of two June 2000 Mw6.5 earthquakes in South Iceland estimated from joint inversion of InSAR and GPS measurements. *Earth Plan. Sci. Lett.* 213, 487-502.

Richwalski, S.M. & F. Roth 2006. Inelastic shear and Coulomb stress changes in the South Iceland seismic zone due to strong earthquakes since 1706. *Tectonophysics,* submitted.

Rivalta, E. & M. Bonafede 2005. Analytical fault and fluid-filled fracture models in viscoelastic media. In: Abstracts of the EGU General Assembly, Vienna, Austria, April 24-29, 2005.

Roth, F. 2004. Stress changes modelled for the sequence of strong earthquakes in the South Iceland seismic zone since 1706. *Pageoph.* 161(7), 1305-1327.

Savage, J.C. & R.O. Burford 1973. Geodetic determination of relative plate motion in central California. *J. Geophys. Res*. 78, 832-845.

Sigmundsson, F., P. Einarsson, R. Bilham & E. Sturkell 1995. Rift-transform kinematics in South Iceland: Deformation from Global Positioning System measurements, 1986 to 1992. *J. Geophys. Res*. 100, 6235-6248.

Slunga, R. 2003. Microearthquake analysis at local seismic networks in Iceland and Sweden and earthquake precursors. In: *Lecture Notes in Earth Sciences.* Methods and Applications of Signal Processing in Seismic Network Operations. Springer Verlag, Germany.

Slunga, R., S.Th. Rögnvaldsson & R. Böðvarsson 1995. Absolute and relative locations of similar events with application to microearthquakes in southern Iceland. *Geophys. J. Int*. 123, 409-419.

Soosalu, H. & P. Einarsson 1997. Seismicity around the Hekla and Torfajökull volcanoes, Iceland, during a volcanically quiet period, 1991-1995. *Bull. Volcanol*. 59, 36-48.

Soosalu, H., P. Einarsson & B.S. Þorbjarnardóttir 2005. Seismic activity associated with the 2000 eruption of Hekla, Iceland. *Bull. Volcanol.* 1432-0819 (online).

Stefánsson R. 1999. A tentative model for the stress build-up and stress release in and around the SISZ. http://hraun.vedur.is/ja/prepared/reports/.
Stefánsson, R. & P. Halldórsson 1988. Strain release and strain build-up in the South Iceland seismic zone. *Tectonophysics* 159, 267-276.

Stefánsson, R., R. Böðvarsson, R. Slunga, P. Einarsson, S.S. Jakobsdóttir, H. Bungum, S. Gregersen, J. Havskov, J. Hjelme & H. Korhonen 1993. Earthquake prediction research in the South Iceland seismic zone and the SIL project. *Bull. Seism. Soc. Am*. 83(3), 696-716.

Stefánsson, R., R. Böðvarsson & G.B. Guðmundsson 1996. Iceland plume tectonics, some speculations and facts. In: B. Þorkelsson (editor), *Seismology in Europe*. Papers presented at the XXV ESC General Assembly, Reykjavík, Iceland, September 9-14, 1996, 505-511.

Stefánsson, R., F. Bergerat, M. Bonafede, R. Böðvarsson, S. Crampin, P. Einarsson, K.L. Feigl, C. Goltz, Á. Guðmundsson, F. Roth, R. Sigbjörnsson, F. Sigmundsson, P. Suhadolc & M. Wyss 2002. Application of practical experience gained from two recent large earthquakes in the South Iceland seismic zone in the context of earthquake prediction research to develop technology for improving preparedness and mitigating risk – PREPARED. An EC proposal. *Veðurstofa Íslands – Greinargerð* 02004. Icelandic Meteorological Office. Report,119 pp.

Stefánsson, R., G.B. Guðmundsson & P. Halldórsson 2003. The South Iceland earthquakes 2000 - challenge for earthquake prediction research. *Veðurstofa Íslands - Greinargerð* 03017. Icelandic Meteorological Office, Report, 21 pp.

Stefánsson, R., & G.B. Guðmundsson 2005. About the state-of-the-art in providing earthquake warnings in Iceland. *Veðurstofa Íslands – Greinargerð* 05003. Icelandic Meteorological Office, Report, 26 pp.

Stefánsson, R. & G.B. Guðmundsson 2006a. Long-term and short-term earthquake warnings based on seismic information in the SISZ. *Veðurstofa Íslands – Greinargerð* 06006. Icelandic Meteorological Office, Report, in press.

Stefánsson, R., & G.B. Guðmundsson 2006b. Ahead of the earthquake: assessment of where, how and when. *Veðurstofa Íslands – Greinargerð*. Icelandic Meteorological Office, Report, in press.

Tryggvason, A., S.Th. Rögnvaldsson & Ó.G. Flóvenz 2002. Three dimensional imaging of the P- and S-wave velocity structure and earthquake locations beneath Southwest Iceland. *Geophys. J. Int*. 151, 848-866.

Tryggvason, K., E. Husebye & R. Stefánsson 1983. Seimic image of the hypothesized Icelandic hot spot. *Tectonophysics* 100, 97-118.

Vogfjörð, K.S. 2003. Triggered seismicity in SW Iceland after the June 17, Mw=6.5 earthquake in the South Iceland Seismic Zone. In: Abstracts of the EGS-AGU-EUG Joint Assembly, Nice, France, April 6-11, 2003.

Wyss, M. & R. Stefánsson 2006. Nucleation points of recent main shocks in southern Iceland mapped by *b*-values. *Bull. Seism. Soc. Am*., accepted.

Zencher, F. & M. Bonafede 2005. Pressure dependent permeability models. In: Abstracts of the EGU General Assembly, Vienna, Austria, April 24-29, 2005.

Zencher, F., M. Bonafede & R. Stefánsson 2006. Near-lithostatic pore pressure at seismogenic depths: a thermo-poroelastic model. *Geophys. J. Int.,* submitted.